Institute for Theoretical Physics
Utrecht University

Master's Thesis

The Swampland Distance Conjecture for Calabi-Yau Fourfold Compactifications

Yannik Zimmermann
mail@yannikzimmermann.de

June 2019

Supervised by Prof. Dr. Thomas Grimm

Abstract

There are a multitude of conjectures about the difference between the space of string theory derivable QFTs – the Landscape – and its complement – the Swampland. One of them, the Swampland Distance Conjecture, states that, upon approaching infinite distance points in field space, an infinite tower of states becomes massless. We study the premise and conclusion of this conjecture for the complex structure moduli space of Calabi-Yau fourfolds. For analyzing infinite distance points we employ the technology of mixed Hodge structures and their Deligne diamonds. With this we are able to give the first known classification of infinite distance divisors for general fourfolds. Furthermore we supplement this with rules for how these divisors can intersect and form an infinite distance network in field space. Using the same technology, we are able to identify infinite towers of states becoming massless for a big class of such intersection patterns. This provides further evidence for the general Swampland Distance Conjecture.

Contents

1 Introduction

1.1 The Swampland and the Distance Conjecture

String theory provides a possible theory of quantum gravity and particle physics at very high energies. In the early stages of its development, physicists were hoping to find a small set of consistent theories and so be able to calculate the free variables of the standard model and other constants of nature from first principles. However, over the last decades it got more and more clear, the number of consistent string vacua is not small, on the contrary, it is truly vast. And each of these vacua produces a different effective quantum field theory at low energies. Trying to find the correct string vacuum reproducing the standard model by pure trial and error became an unfeasible task. So, in the early 2000s, researchers started to pursue a new strategy. By studying which low energy theories can possibly emerge from string theory (or quantum gravity in general) they hope to get a better understanding of the theories as a whole. In the course of this program, a new border in the space of quantum field theories was drawn, separating the *Landscape* from the *Swampland*. The Landscape includes all field theories that are the low energy limit of some string vacuum, whereas the Swampland contains all theories that do not come out of such a limit. Cartographing this border turns out to be a complicated task and at the moment there are a multitude of conjectures about it with varying degree of evidence. Some examples are the weak gravity conjecture, the de Sitter conjecture or the distance conjecture; a review of the latest research can be found in [1]. For the scope of this thesis I am going to concentrate on the latter: the *Swampland Distance Conjecture*, SDC for short, first proposed by Ooguri and Vafa [2]. In its general form it states:

Swampland Distance Conjecture. *Consider a QFT, coupled to gravity, with field space $\mathcal{M}$, i.e. the space that the fields take their value in. Suppose that there exists a point $P \in \mathcal{M}$ such that for any point other point $Q \in \mathcal{M}$ their geodesic distance, denoted $d(Q, P)$, is infinite. Then there exists an infinite tower of states, with an associated mass m depending on the point in field space, such that for $P' \in \mathcal{M}$ approaching P, i.e. $P' \to P$,*

$$m(P') \sim m(Q)\mathrm{e}^{-\alpha d(P',Q)}\,, \tag{1.1}$$

where α is some positive constant.

The conjecture received a lot of attention recently [3–14]. It seems to be interconnected with other Swampland conjectures, for example, the weak gravity conjecture [3, 4] or the de Sitter conjecture [5] and forms therefore an important building block in the understanding of the swampland program and string theory as a whole. The insights gained so far led for example to the proposal that infinite distances in field space and the infrared dynamics of fields in general emerge from integrating out towers of states in the ultraviolet [5, 6]. Further, on a more practical note, it gives us more information about the difficulties of realizing large field inflation within string derived models [7]. This also inspired the formulation of the Refined Swampland Distance Conjecture, which extends the statement to super-Planckian, but still finite, field distances [8–10].

The SDC was shown to hold for supergravity theories with more than 8 supercharges in any dimension [11]. In theories with less supercharges, for example Calabi-Yau threefold compactifications of type IIB string theory, strong evidence was found by [6] using the powerful mathematics of Hodge theory. This analysis was extended from one-parameter approaches to infinite distance to multi-parameter approaches in [12]. Building on this work, I will in this thesis repeat the same analysis for Calabi-Yau fourfolds. Fourfolds play an important role in connecting the twelve-dimensional physics of F-theory to our apparently four-dimensional world. But because handling F-theory in the low energy limit is difficult, we will only look at fourfold compactifications of type IIA string theory from ten to two dimensions. The important details of this will be repeated in section 1.5. However, the results of the analysis do only really depend on the properties of the Calabi-Yau, so a generalization to other scenarios is easily possible.

Stated concretely, we will analyze and classify singular divisors in the complex structure moduli space of fourfolds with the help of mixed Hodge structures in the first half of chapter 2. The given classification can be used to state whether points on the divisors lie at infinite distance or not. Further we provide criteria for which divisors can intersect and form an infinite distance network in moduli space in the second half of chapter 2. Following this we try to identify infinite and massless towers of states at infinite distance points in chapter 3. We will look at arbitrary intersection patterns of different divisors and successfully identify the towers in form of charge orbits of BPS D-branes for a big family of patterns. This provides strong evidence for the SDC for Calabi-Yau fourfold compactifications.

But first, in the rest of this chapter, we will discuss the compactification of a string on a circle to provide a first example and evidence for the SDC, and after that introduce Calabi-Yau manifolds and their compactification.

1.2 A brief reminder of superstring theory

Superstring theory describes the movement of a one-dimensional string with fermionic degrees of freedom through spacetime. The excitations of this string are massless and massive oscillator modes, which will correspond to massless and massive particles after taking the low energy limit and connecting with ordinary particle physics. Because the massive excitations are expected to have masses around the Planck scale, we only consider the massless modes when taking this limit. There are only five types of superstrings, denoted by type I, IIA, IIB and two different heterotic ones. All of these have to live in ten dimensions. So, if we want to make a connection with our four-dimensional spacetime, we need to follow a compactification procedure. The idea of this is that the extra dimensions are compact, i.e. “curled up”, so that on big length scales they cannot be detected. There are now two possibilities for when to compactify. On the one hand, we can first compactify the ten-dimensional spacetime of the superstring and take the low energy limit after that. This procedure gives more complete results, because it takes winding modes into account (these will be explained further below). On the other hand, we can first take the low energy limit and compactify spacetime only after that. This approach has the advantage of being easier to calculate, but ignores stringy effects, like winding modes.

We will discuss in the next section the first case to find first evidence for the SDC. After that we turn to the second case and introduce the main subject of this thesis: Calabi-Yau compactifications.

1.3 Infinite massless towers from a string on $M_9 \times S^1$

Let us discuss the compactification of a bosonic string on a circle as a first example providing motivation for the SDC. The discussion is an abbreviated form of the one found in [1]. We take spacetime to look like $M_{10} = M_9 \times S^1$ with coordinates $X^M = (X^\mu, X^9)$, where $\mu = 0, \dots, 8$ and $X^9 \cong X^9 + 1$. The metric takes the form

$$\mathrm{d}s^2 = \mathrm{e}^{2\alpha\phi(X^\mu)} g_{\mu\nu}(X^\mu)\, \mathrm{d}X^\mu\, \mathrm{d}X^\nu + \mathrm{e}^{-2\beta\phi(X^\mu)} \big(\mathrm{d}X^9\big)^2 \,, \tag{1.2}$$

where α and β are positive constants and $\phi(X^\mu)$ is a background scalar field that parametrizes the radius R of the compact dimension at each point X^μ:

$$2\pi R(X^\mu) \equiv \mathrm{e}^{\beta\phi(X^\mu)} \,. \tag{1.3}$$

The field space of ϕ is $\mathcal{M}_\phi = (-\infty, +\infty)$.

Strings moving in this background get two extra quantum numbers. The first one parametrizes the quantized momentum in the compact dimension X^9:

$$p^9 = \frac{n}{R} \quad \text{with } n \in \mathbb{Z} \,. \tag{1.4}$$

The second quantum number appears because strings are extended objects and can therefore wrap around the compact dimension $w \in \mathbb{Z}$ times; see fig. 1.1 for an illustration. Taking both possibilities into account, the nine dimensional mass for the string ground state, i.e. with no oscillators excited, is given by

$$\Big(m_{n,w}\Big)^2 = \Big(2\pi \mathrm{e}^{\gamma\phi} n\Big)^2 + \Big(\frac{1}{2\pi\alpha'} \mathrm{e}^{-\gamma\phi} w\Big)^2 \tag{1.5}$$

where $\gamma = \alpha + \beta > 0$.

If we look now at the nine dimensional effective theory, we can see that there are two infinite towers of massive states. A tower of momentum modes, with masses given by $m_{n,0}$ and a tower of winding modes, with masses given by $m_{0,w}$. Each tower has a mass scale that multiplicates the integers n and w respectively:

$$m_n \sim \mathrm{e}^{\gamma\phi} \qquad m_w \sim \mathrm{e}^{-\gamma\phi} \,. \tag{1.6}$$

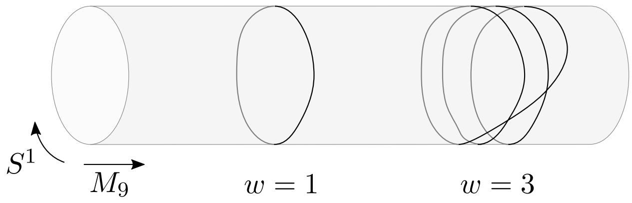

Figure 1.1: Two strings winding around the compactified dimension.

It is now easy to identify the Distance Conjecture: For any two values $\phi_1, \phi_2 \in \mathcal{M}_\phi$ there exists an infinite tower of states, with some mass scale m, which becomes light exponentially in $|\phi_1 - \phi_2|$:

$$m(\phi_2) \sim m(\phi_1)\mathrm{e}^{-\gamma|\phi_1-\phi_2|}\,. \tag{1.7}$$

The tower of states becoming light is the momentum tower if $\phi_1 - \phi_2 < 0$ while it is the winding tower if $\phi_1 - \phi_2 > 0$. So there is always some tower that becomes light, even though the states it is composed of change. The winding modes (which are string-theoretic) are very important for this fact; without them we would not have found the conjectured behavior.

With this example we also see why the SDC is interesting. If we send one of the ϕ_i to $\pm\infty$, then an infinite number of states becomes massless, which means that the description as a nine dimensional quantum field theory breaks down at these infinite distance points.

Lastly, note that the field ϕ approaching infinite distance is a moduli of the circle, i.e. it parametrizes its geometry. The same will also happen later in our discussion of Calabi-Yau compactifications. There too, it will be the moduli that approach infinite distance.

With this example we are now having a first motivation and evidence for the SDC. The behavior carries over to compactifications with products of circles, i.e. with tori, but because these preserve a large number of supersymmetry ($\mathcal{N} = 8$ for a T^6 compactification) we need to look at more complicated manifolds if we want a more realistic scenario.

1.4 A brief introduction to Calabi-Yau manifolds

I present here a brief introduction to Calabi-Yau manifolds, closely following [15]; more details can be found there. We are interested in Calabi-Yau compactifications, because we want to preserve a small amount of supersymmetry to keep some control in the low dimensional theory. To find a supersymmetric vacuum state we need a covariantly constant spinor η, i.e. $\nabla_M \eta = 0$, on the internal manifold. This condition leads us exactly to Calabi-Yau manifolds, which preserve $\mathcal{N} = 2$ supersymmetry. In this section we will present these, following however a different definition, namely as Kähler manifolds with first Chern class equal to zero.

Let us start with introducing Kähler manifolds, which are complex and symplectic manifolds.

A *complex manifold* of (complex) dimension n (and real dimension $2n$) is a manifold that locally looks like $\mathbb{C}^n$. We denote the coordinates of a chart by z^i. The complexified cotangent bundle splits into a holomorphic and antiholomorphic part with basis elements $\mathrm{d}z^i$ and $\mathrm{d}\bar{z}^{\bar{\jmath}}$ respectively. A differential form is then said to be of type (p,q) if it can be written as

$$A_{p,q} = \frac{1}{p!q!} A_{i_1 \dots i_p \bar{\jmath}_1 \dots \bar{\jmath}_q} \mathrm{d}z^{i_1} \wedge \dots \wedge \mathrm{d}z^{i_p} \wedge \mathrm{d}\bar{z}^{\bar{\jmath}_1} \wedge \dots \wedge \mathrm{d}\bar{z}^{\bar{\jmath}_q} \ . \tag{1.8}$$

Similarly, the exterior derivative splits into a holomorphic and an antiholomorphic piece, namely $\mathrm{d} = \partial + \bar{\partial}$, where

$$\partial \colon (p,q) \to (p+1,q) \ , \qquad \bar{\partial} \colon (p,q) \to (p,q+1) \ . \tag{1.9}$$

A *symplectic manifold* has $2n$ real dimensions and exhibits a globally defined, nowhere vanishing, closed two-form J, that is non-degenerate, i.e. the top-form J^n is nowhere vanishing. Such manifolds exhibit so called Darboux coordinates (x^i, y^i) in which

$$J = \sum_{i=1}^{n} \mathrm{d}x^i \wedge \mathrm{d}y^i \ . \tag{1.10}$$

A *Kähler manifold* is now a complex and symplectic manifold with compatible complex and symplectic structure. This means that J is a $(1,1)$-form, i.e. $J = J_{i\bar{\jmath}} \mathrm{d}z^i \wedge \mathrm{d}\bar{z}^{\bar{\jmath}}$. With this it is also possible to define a hermitian metric, derived from a real scalar function K, called the Kähler potential:

$$g_{i\bar{\jmath}} = -\mathrm{i} J_{i\bar{\jmath}} = \partial_i \bar{\partial}_{\bar{\jmath}} K \ . \tag{1.11}$$

Another important aspect of Kähler manifolds is their cohomology. On complex manifolds we can define cohomology classes for (p,q)-forms, similar to the regular p-form de Rham cohomology classes for normal manifolds. On Kähler manifolds now it doesn't matter which of the derivatives, d, ∂ or $\bar{\partial}$, we use:

$$H^{p,q}_{\mathrm{d}} = H^{p,q}_{\partial} = H^{p,q}_{\bar{\partial}} \ . \tag{1.12}$$

The dimensions of the cohomology classes are denoted by the Hodge numbers $h^{p,q} = \dim H^{p,q}$ and satisfy the symmetry relation

$$h^{p,q} = h^{q,p} = h^{n-p,n-q} \ . \tag{1.13}$$

The numbers are usually arranged in the form of a Hodge diamond

$$\begin{array}{ccccccccc} & & & & h^{0,0} & & & & \\ & & & h^{1,0} & & h^{0,1} & & & \\ & & h^{2,0} & & h^{1,1} & & h^{0,2} & & \\ & h^{3,0} & & h^{2,1} & & h^{1,2} & & h^{0,3} & \\ h^{4,0} & & h^{3,1} & & h^{2,2} & & h^{1,3} & & h^{0,4} \\ & h^{4,1} & & h^{3,2} & & h^{2,3} & & h^{1,4} & \\ & & h^{4,2} & & h^{3,3} & & h^{2,4} & & \\ & & & h^{4,3} & & h^{3,4} & & & \\ & & & & h^{4,4} & & & & \end{array} \ , \tag{1.14}$$

which is symmetric under reflections along the horizontal and vertical axis (due to eq. (1.13)).

This brings us to the last ingredient for Calabi-Yau manifolds. We need the *first Chern class*, which is the cohomology class of the Ricci two-form. This two-form is defined as

$$\mathcal{R} = -\mathrm{i}\partial\bar{\partial}\log\det(g_{i\bar{\jmath}}) \tag{1.15}$$

and it is closed on Kähler manifolds, i.e. $\mathrm{d}\mathcal{R} = 0$. We can therefore take its cohomology class and call it first Chern class

$$c_1 = \frac{1}{2\pi}[\mathcal{R}]\,. \tag{1.16}$$

A *Calabi-Yau n-fold* can now be defined as an n complex dimensional Kähler manifold with $c_1 = 0$. Working out the Hodge numbers for, for example, a fourfold we get the Hodge diamond

$$\begin{array}{ccccccccc}
 & & & & 1 & & & & \\
 & & & 0 & & 0 & & & \\
 & & 0 & & h^{1,1} & & 0 & & \\
 & 0 & & h^{2,1} & & h^{2,1} & & 0 & \\
1 & & h^{3,1} & & h^{2,2} & & h^{3,1} & & 1 \\
 & 0 & & h^{2,1} & & h^{2,1} & & 0 & \\
 & & 0 & & h^{1,1} & & 0 & & \\
 & & & 0 & & 0 & & & \\
 & & & & 1 & & & &
\end{array}\,. \tag{1.17}$$

Note that due to the symmetries from eq. (1.13) we are only left with four independent variables. This number gets further reduced by the relation [16]

$$h^{2,2} = 2(22 + 2h^{1,1} + 2h^{3,1} - h^{2,1})\,. \tag{1.18}$$

Lastly, two more definitions that will play an important role later: Firstly, from the cohomology class $H^{4,0}$, which is one-dimensional, one picks a representative Ω and calls it the holomorphic four-form. Secondly, on the middle cohomology $H^4 = H^{4,0} + H^{3,1} + H^{2,2} + H^{1,3} + H^{0,4}$ we can define an antisymmetric product S (and its matrix form η with respect to some basis)

$$S(v,w) = \int_{Y_4} v \wedge w \equiv \mathbf{v}^{\mathsf{T}}\eta\,\mathbf{w} \quad \text{for } v,w \in H^4 \tag{1.19}$$

and further the Hodge inner product

$$\langle v|w\rangle = \int_{Y_4} v \wedge \star\overline{w} \quad \text{for } v,w \in H^4\,, \tag{1.20}$$

where $\star$ denotes the Hodge star.

1.5 Compactifying type IIA theory on Calabi-Yau fourfolds

We are now going to discuss the fourfold compactification of type IIA string theory after taking the low energy limit. This limit turns out to be type IIA supergravity in ten dimensions. I want to remind that we are mainly interested in the general properties of the fourfold and that the details of type IIA theory are of secondary importance. Because of this, we will only be interested in the gravitational sector, i.e. in the behavior of the metric under compactification. Its action is given by [17]

$$\mathcal{S}^{(10)}_{\mathrm{IIA,grav}} = \frac{1}{2}\int_{M_{10}} \mathrm{d}^{10}x\,\sqrt{-g^{(10)}}\mathrm{e}^{-2\Phi^{(10)}} R^{(10)} \tag{1.21}$$

where $g^{(10)}_{MN}$ is the ten-dimensional metric, $R^{(10)}$ its scalar curvature and $\Phi^{(10)}$ the ten-dimensional dilaton.

The recipe for a Kaluza-Klein compactification is now to make a product ansatz for the spacetime manifold

$$M_{10} = M_2 \times Y_4\,, \tag{1.22}$$

where for our purposes we picked a Calabi-Yau fourfold as the compact internal manifold. Next, we expand the metric as a fluctuation around the ground state

$$g^{(10)}_{MN} = \begin{pmatrix} g^{(2)}_{\mu\nu} & \\ & g^{(8)}_{ab} \end{pmatrix} \tag{1.23}$$

with some arbitrary two-dimensional metric $g^{(2)}_{\mu\nu}$ and a fixed Calabi-Yau metric $g^{(8)}_{ab}$. The fluctuations are then expanded in eigenfunctions of the mass operator on the Calabi-Yau. For the metric this looks for example like

$$\delta g_{ab}(x,y) = \sum_n X^{(n)}(x) Y^{(n)}_{ab}(y)\,, \tag{1.24}$$

The x-dependent coefficient functions $X^{(n)}$ appear as fields in the two-dimensional theory whose masses are given by the eigenvalues of the eigenfunctions $Y^{(n)}$. In the Kaluza-Klein approximation we ignore now all the massive fields and consider only the massless ones. In particular this means that the moduli of the metric of the internal manifold appear as massless fields in the low-dimensional effective theory. With moduli we mean the parameters of possible deformations that keep the general structure intact. For Calabi-Yau fourfolds these are given by $h^{3,1}$ complex variables Z^α parametrizing the complex structure and by $h^{1,1}$ real variables M^A parametrizing the Kähler structure. The moduli Z^α and M^A form now the so called moduli space, which parametrizes the smooth deformations of the ground state Calabi-Yau. For each point in this moduli space we get an associated Calabi-Yau manifold.

Plugging the expansions into the ten-dimensional action of eq. (1.21) and performing the integral over the Calabi-Yau we get the two-dimensional effective action [17]

$$\mathcal{S}^{(2)}_{\mathrm{IIA,grav}} = \int_{M_2} \mathrm{d}^2x\,\sqrt{-g^{(2)}}\mathrm{e}^{-2\Phi^{(2)}}\left(\frac{1}{2}R^{(2)} - G_{\alpha\bar\beta}\partial_\mu Z^\alpha \partial^\mu \bar Z^{\bar\beta} - G_{AB}\partial_\mu M^A \partial^\mu M^B\right) \tag{1.25}$$

with two dimensional scalar curvature $R^{(2)}$ and dilaton $\Phi^{(2)}$. The main point to note here are the two kinetic terms for the complex structure and Kähler moduli. The two terms don't mix, which means that the moduli space is a product space of the complex structure moduli space $\mathcal{M}_{\text{cs}}$ and the Kähler moduli space $\mathcal{M}_{\text{K}}$. For the rest of this thesis we are going to concentrate on the complex structure moduli space $\mathcal{M} \equiv \mathcal{M}_{\text{cs}}$. It is $h^{3,1}$ complex dimensional, comes equipped with a metric $G_{\alpha\bar{\beta}}$ and even turns out to be Kähler itself. This means the metric can be derived from a Kähler potential

$$G_{\alpha\bar{\beta}} = \partial_{Z^\alpha} \bar{\partial}_{\bar{Z}^{\bar{\beta}}} K \tag{1.26}$$

$$K = -\ln\left(\int_{Y_4} \Omega \wedge \overline{\Omega}\right) \tag{1.27}$$

Scope of this thesis is now to provide further evidence for the SDC for these fourfold compactifications. The fields and field space mentioned at the beginning will be the complex structure and their moduli space $\mathcal{M}$; the metric for measuring distances will be the one from eq. (1.26). Our strategy will be to identify in the next chapter the infinite distance points as singular points in $\mathcal{M}$ and after that try to construct infinite towers of BPS D-brane states becoming massless in chapter 3.

2 The singularity structure of Calabi-Yau fourfold moduli space

The moduli space of Calabi-Yau manifolds has singular points at which the corresponding Calabi-Yau becomes degenerate. These singular points are the natural candidates for the infinite distance points of the Distance Conjecture. Our goal in this chapter is therefore to get a better understanding of the global picture of these singular points in Calabi-Yau fourfold complex moduli space. In section 2.2 we will first start a classification of individual points as a local analysis and later then, in section 2.4, we will look at how different points are connected. There, a global structure starts to emerge. Thereby we will make use of the middle cohomology $H^4(Y_4)$ of the Calabi-Yau and the monodromy in moduli space around the singular points. This helps us to analyze the degeneration with tools from algebraic geometry, which we will introduce in section 2.1.

The middle cohomology $H^4 \equiv H^4(Y_4)$ splits due to the Hodge splitting by the complex structure into smaller subspaces. This splitting defines a *Hodge stucture*, which varies together with the Y_4 over the moduli space and degenerates at the singular points. However, it turns out that H^4 splits into a finer splitting, a *mixed Hodge structure*, which doesn't become degenerate at these points.

With this avatar of our main character H^4 we are equipped to answer the question: What kind of singular points does the moduli space have? Are they all the same or can we find a distinction?

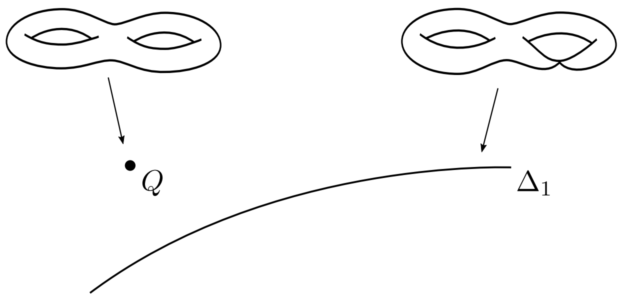

Figure 2.1: The moduli space of a two-torus with a generic point Q and a singular divisor Δ_1.

2.1 Analyzing singularities with mixed Hodge structures

Our strategy for answering this question of the classification of singular points is to first introduce the powerful technology of mixed Hodge structures (following [18]) and then to use it to transform the problem into one that is easier to solve.

The Hodge decomposition of the middle cohomology of a Calabi-Yau n-fold

$$H^n = \bigoplus_{p+q=n} H^{p,q} \quad \text{such that} \quad \overline{H^{p,q}} = H^{q,p} \tag{2.1}$$

defines a *Hodge structure of weight* n on the vector space $H^n(Y_n)$. The bilinear form S from eq. (1.19) gives a *polarization* on the Hodge structure, meaning that

$$S(H^{p,q}, H^{r,s}) = 0 \quad \text{for } p \neq s, q \neq r \tag{2.2}$$

$$\mathrm{i}^{p-q} S(v, \bar{v}) > 0 \quad \text{for } v \in H^{p,q}, v \neq 0\,. \tag{2.3}$$

As we move around in the complex structure moduli space, the complex structure and therefore the Hodge structure it induces changes. This leads to a *variation of Hodge structure*; the $H^{p,q}$ from eq. (2.1) look different for each point in moduli space, even though the total H^n stays the same. The complex structure moduli space of Calabi-Yau manifolds is neither smooth nor compact; it can have singular points at which the associated manifold becomes degenerate. We now want to find out what happens to the Hodge structure as we approach such singular points. We already mentioned that it becomes singular itself, but it turns out that this happens in a very predictable manner, allowing us to recover a structure that is well defined at the singular point: a *mixed Hodge structure.*

The singular points in moduli space form a locus Δ which can be written as $\Delta = \bigcup_i \Delta_i$, where the Δ_i are smaller normally intersecting loci. We will introduce a shorthand notation for the intersection of these loci

$$\Delta_{i_1\dots i_k} \coloneqq \Delta_{i_1} \cup \dots \cup \Delta_{i_k} \tag{2.4}$$

$$\Delta_{(k)} \coloneqq \Delta_{1\dots k} \tag{2.5}$$

$$\Delta^\circ_{i_1\dots i_k} \coloneqq \Delta_{i_1\dots i_k} - \bigcup_{m\neq i_1,\dots,i_k} \Delta_{i_1\dots i_k m}\,. \tag{2.6}$$

We will use the notation with an index in parentheses also for other objects to indicate a combination of objects with indices up to the enclosed index. The last definition denotes the part of the locus that is not part of any higher intersection.

We will denote the singular point we are concentrating on always with P. The number of intersecting loci it lies on is denoted with n_P, i.e. $P \in \Delta_{(n_P)}$ after a suitable renaming of the loci. Besides that, however, we allow a total of $n_\mathcal{E}$ intersecting loci in the neighborhood of P. For getting information about all singular points of Δ we will analyze them using a local perspective to get a general description. We choose a coordinate system on a patch of the moduli space such that P lies at $z_i = 0$ for $i = 1, \dots, n_P$. The remaining z_j, $j = n_P + 1, \dots, h^{3,1} = \dim(\mathcal{M})$ can be arbitrary and won't play any role in the following discussion. The coordinates can therefore be thought of coming from the product of $h^{3,1} - n_P$ disks $\mathbb{D} = \{z \in \mathbb{C} \mid |z| < 1\}$ and n_P punctured disks $\mathbb{D}^* = \mathbb{D} - \{0\}$. We have $(z_i, z_j) \in (\mathbb{D}^*)^{n_P} \times \mathbb{D}^{h^{3,1}-n_P}$. Each of the coordinates z_i has a monodromy matrix T_i associated to it. It describes how a differential form in H^n transforms as we go around the origin in the respective complex plane once (by sending $z_i \to \mathrm{e}^{2\pi \mathrm{i}} z_i$). It must not necessarily be the unit matrix. One can show that the monodromy matrices are quasi unipotent, i.e. they satisfy $(T^m - \mathbb{1})^{n+1} = 0$ for some positive integers m and n. For the following discussions we extract the relevant nilpotent part by defining the monodromy logarithms

$$N_i = \frac{1}{m_i} \ln(T_i^{m_i}) \,, \tag{2.7}$$

where m_i and n_i (used in the next equation) are the smallest integers satisfying $(T_i^{m_i} - \mathbb{1})^{n_i+1} = 0$. From the definition it follows that the monodromy logarithms are nilpotent

$$N_i^{n_i+1} = 0 \,. \tag{2.8}$$

With the information about the structure of the Calabi-Yau – in form of its Hodge structure – and the information about the singularities – in form of the monodromy logarithms – we can now try to simplify the problem of classification. A first step is to use a theorem stating that the Hodge structure becomes a *mixed Hodge structure* at every singular point. Such a mixed Hodge structure gives a finer splitting of H^n, not just into spaces $H^{p,q}$ with $p+q=n$, but instead into spaces $I^{p,q}$ with $p, q \leq n$:

$$H^n = \bigoplus_{0 \leq p,q \leq n} I^{p,q} \,. \tag{2.9}$$

For fourfolds ($n = 4$) this gives for example

$$H^{4,0}\quad H^{3,1}\quad H^{2,2}\quad H^{1,3}\quad H^{0,4} \qquad \xrightarrow{\text{move to } P} \qquad \begin{array}{ccccccccc} &&&&I^{4,4}&&&& \\ &&&I^{4,3}&&I^{3,4}&&& \\ &&I^{4,2}&&I^{3,3}&&I^{2,4}&& \\ &I^{4,1}&&I^{3,2}&&I^{2,3}&&I^{1,4}& \\ I^{4,0}&&I^{3,1}&&I^{2,2}&&I^{1,3}&&I^{0,4} \\ &I^{3,0}&&I^{2,1}&&I^{1,2}&&I^{0,3}& \\ &&I^{2,0}&&I^{1,1}&&I^{0,2}&& \\ &&&I^{1,0}&&I^{0,1}&&& \\ &&&&I^{0,0}&&&& \end{array} \,. \tag{2.10}$$

How are these $I^{p,q}$ now defined? Of course they should depend on the two input data. For their dependence on the Hodge structure, we first have to reassemble the spaces $H^{p,q}$ into more well behaved objects. We introduce the *Hodge filtration*,

$$F^p = \bigoplus_{p' \geq p} H^{p', n-p'} \,, \tag{2.11}$$

which becomes for the case $n = 4$

$$\begin{aligned} &F^4 = H^{4,0} \\ &\cap \\ &F^3 = H^{4,0} + H^{3,1} \\ &\cap \\ &F^2 = H^{4,0} + H^{3,1} + H^{2,2} \\ &\cap \\ &F^1 = H^{4,0} + H^{3,1} + H^{2,2} + H^{1,3} \\ &\cap \\ &F^0 = H^{4,0} + H^{3,1} + H^{2,2} + H^{1,3} + H^{0,4} \, . \end{aligned} \tag{2.12}$$

These complex spaces vary holomorphically with the complex structure moduli z_i. Nevertheless, just like the $H^{p,q}$, the F^p become degenerate as we move to Δ. It is possible though to show that

$$F^p(\Delta_{(n_P)}) = \lim_{t_1,\dots,t_{n_P}\to+\mathrm{i}\infty} \exp(-\textstyle\sum_{i=1}^{n_P} t_i N_i) F^p \tag{2.13}$$

is well behaved. Here we defined the coordinates

$$t_i \equiv x_i + \mathrm{i} y_i = \frac{1}{2\pi\mathrm{i}} \ln z_i \, . \tag{2.14}$$

Further the "orthogonality"[1] property eq. (2.2) becomes

$$S(F^p, F^{n+1-p}) = 0 \, . \tag{2.15}$$

Lastly, note that Ω spans the one-dimensional F^n; we will denote the corresponding limiting element spanning $F^n(\Delta_{(n_P)})$ with $\mathbf{a}_0$, i.e.

$$\mathbf{a}_0 = \lim_{t_1,\dots,t_{n_P}\to+\mathrm{i}\infty} \exp(-\textstyle\sum_{i=1}^{n_P} t_i N_i)\Omega \, . \tag{2.16}$$

The limiting filtration $F^p(\Delta_{(n_P)})$ is now our first input for the mixed Hodge structure.

The second input is another filtration, the *monodromy filtration* W_l, this time directly extracted from the N_i. First, for the case that we want to move to the intersection of multiple divisors Δ_i, we need to combine the N_i into one object. We take a linear combination $\sum_{i=1}^{n_P} c_i N_i$ and one can show that the wanted filtration W_l don't depend on the choice of the c_i, as long as $c_i > 0$. We thus pick the most convenient combination and use

$$N_{(n_P)} \equiv N_1 + \cdots + N_{n_P} \, . \tag{2.17}$$

The monodromy filtration $W_l \equiv W_l^{(n_P)}$ is now obtained from the images and kernels of $N \equiv N_{(n_P)}$ and its powers with the general formula

$$W_l = \bigoplus_{\substack{k\geq 1 \\ k \geq l-n+1}} \ker N^k \cap \operatorname{im} N^{k-l+n-1} \tag{2.18}$$

[1] Note that S is symmetric (antisymmetric) for n even (odd).

and the use of $N^{n+1} = 0$. For $n = 4$ this becomes

$$\begin{aligned}
&W_0 = \operatorname{im} N^4 \\
&\cap \\
&W_1 = \ker N \cap \operatorname{im} N^3 \\
&\cap \\
&W_2 = \operatorname{im} N^3 + \ker N \cap \operatorname{im} N^2 \\
&\cap \\
&W_3 = \ker N^2 \cap \operatorname{im} N^2 + \ker N \cap \operatorname{im} N \\
&\cap \\
&W_4 = \operatorname{im} N^2 + \ker N^2 \cap \operatorname{im} N + \ker N \\
&\cap \\
&W_5 = \ker N^3 \cap \operatorname{im} N + \ker N^2 \\
&\cap \\
&W_6 = \operatorname{im} N + \ker N^3 \\
&\cap \\
&W_7 = \ker N^4 \\
&\cap \\
&W_8 = H^4 \,.
\end{aligned} \tag{2.19}$$

Again we have an "orthogonality" relation

$$S(W_{n+l}, W_{n-l-1}) = 0 \,. \tag{2.20}$$

With $F_\Delta \equiv F(\Delta_{(n_P)})$ we have now all the data for defining the finer splitting of the mixed Hodge structure:

$$I^{p,q} = F^p_\Delta \cap W_{p+q} \cap \left(\bar{F}^q_\Delta \cap W_{p+q} + \sum_{j\geq 1} \bar{F}^{q-j}_\Delta \cap W_{p+q-j-1} \right) . \tag{2.21}$$

This definition is chosen because it has the unique properties

$$F^p_\Delta = \bigoplus_{r\geq p} \bigoplus_{s} I^{r,s} \,, \qquad W_l = \bigoplus_{p+q\leq l} I^{p,q} \,, \qquad \bar{I}^{p,q} = I^{q,p} \mod \bigoplus_{\substack{r<q \\ s<p}} I^{r,s} \,. \tag{2.22}$$

The first two relations are visualized in fig. 2.2. From the definition follows also the crucial relation

$$N I^{p,q} \subset I^{p-1,q-1} \tag{2.23}$$

and combining eqs. (2.15) and (2.20) gives

$$S(I^{p,q}, I^{r,s}) = 0 \quad \text{unless } p + r = q + s = n \,. \tag{2.24}$$

For later use we define the graded spaces

$$Gr_{n+l} = \bigoplus_{p+q=n+l} I^{p,q} \,. \tag{2.25}$$

One can show that N^l provides an isomorphism from Gr_{n+l} to Gr_{n-l}.

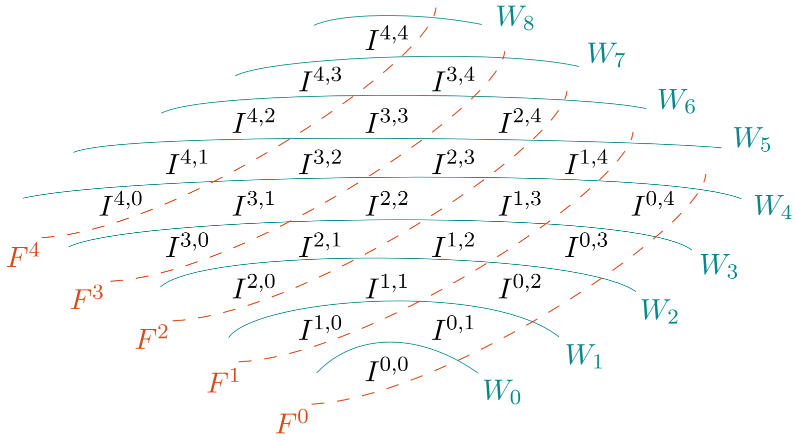

Figure 2.2: Visualization of eq. (2.22) of how to recover F^p_Δ and W_l from the Deligne splitting.

The last relation in eq. (2.22) is important to note; it marks a difference to Hodge structures and complicates many calculations. There is however a special basis for H^n in which $\bar{I}^{p,q} = I^{q,p}$ and the N_i become N_i^- which are members of mutually commuting $\mathfrak{sl}_2$triplets [19]. For a detailed review and explicit example we refer to [12]. We will explain more properties of the N_i^- as soon as we need them.

For the last step in transforming our problem of the classification of singular points it is important to stress that each singular point $P \in \Delta$ has a potentially different Deligne splitting assigned to it. The next step is now to only look at the dimensions of the spaces $I^{p,q}$ assigned to P. This gives us the so called *Deligne diamonds* and one can prove that mixed Hodge structures are up to automorphisms classified by these diamonds.

2.2 Classifying singularities with Deligne diamonds

The *Deligne diamond* of a mixed Hodge structure is given by its *Deligne numbers*. For $n = 4$ it looks like

$$\begin{array}{ccccccccc} & & & & i^{4,4} & & & & \\ & & & i^{4,3} & & i^{3,4} & & & \\ & & i^{4,2} & & i^{3,3} & & i^{2,4} & & \\ & i^{4,1} & & i^{3,2} & & i^{2,3} & & i^{1,4} & \\ i^{4,0} & & i^{3,1} & & i^{2,2} & & i^{1,3} & & i^{0,4} \\ & i^{3,0} & & i^{2,1} & & i^{1,2} & & i^{0,3} & \\ & & i^{2,0} & & i^{1,1} & & i^{0,2} & & \\ & & & i^{1,0} & & i^{0,1} & & & \\ & & & & i^{0,0} & & & & \end{array} \;, \qquad i^{p,q} = \dim_{\mathbb{C}} I^{p,q} \,. \tag{2.26}$$

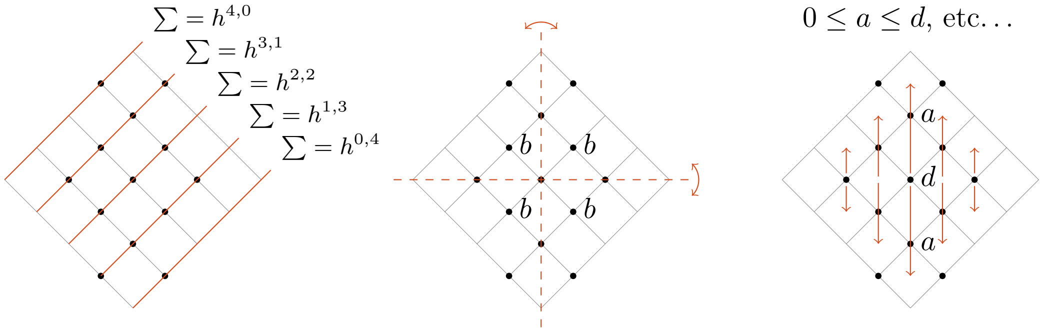

(a) Equation (2.28) **(b)** Equation (2.29) **(c)** Equation (2.30)

Figure 2.3: Visualization of the properties of Deligne diamonds: (a) rows sum to Hodge numbers $h^{p,q}$, (b) mirror symmetry along two axes, (c) the $i^{p,q}$ do not increase when going away from the horizontal diagonal. A type IV diamond with some indices suppressed is used for the examples.

For these diamonds we introduce a graphical notation, illustrated with the following example

$$\begin{array}{ccccccccc} & & & & 0 & & & & \\ & & & 1 & & 1 & & & \\ & & 0 & & a & & 0 & & \\ & 0 & & b & & b & & 0 & \\ 0 & & c & & d & & c & & 0 \\ & 0 & & b & & b & & 0 & \\ & & 0 & & a & & 0 & & \\ & & & 1 & & 1 & & & \\ & & & & 0 & & & & \end{array} \quad \cong$$

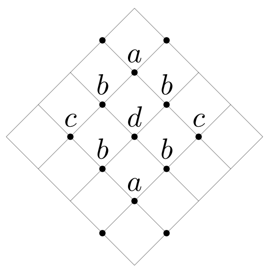

. (2.27)

Here, a label at a dot at (p, q) represents the value of $i^{p,q}$, a dot without label represents the value 1 and no dot represents 0.

Due to the way the Deligne splitting is constructed, the $i^{p,q}$ fulfill the properties

$$h^{p,n-p} = \sum_{q=0}^{n} i^{p,q} \qquad p = 0, \ldots, n \tag{2.28}$$

$$i^{p,q} = i^{q,p} = i^{n-p,n-q} \qquad \text{for all } p, q \tag{2.29}$$

$$i^{p,q} \geq i^{p-1,q-1} \qquad \text{for } p + q \leq n\,, \tag{2.30}$$

where $h^{p,n-p}$ are the Hodge numbers of H^n. Figure 2.3 visualizes these equations.

These very manageable properties give us now a way to classify all possible Deligne diamonds. This, in turn, gives a classification of mixed Hodge structures and therefore also of singular points. The way how we approach this classification is by exploiting that fourfolds have $h^{4,0} = 1$, i.e. the Hodge numbers of H^4 are just $\mathbf{h} = (1, h^{3,1}, h^{2,2}, h^{3,1}, 1)$. This simplifies the task considerably, because it means that eq. (2.28) with $p = 4$ becomes just $1 = \sum_{q=0}^{4} i^{4,q}$, i.e. the top-left row sums to 1. Due to the $i^{p,q}$ being non-negative it follows that one of the $i^{4,q}$ is 1 and the rest is 0, i.e. there is only one dot in the top-left row. This results in five distinct cases, where respectively $i^{4,q} = \delta_{qd}$ with $d = 0, 1, 2, 3, 4$. We label these cases by Latin numerals I, II, III, IV, V (following the convention of [20]).

By the symmetry of eq. (2.29) this fixes the outermost Deligne numbers for each type, whereas the inner nine numbers stay undetermined by this but get reduced down to four independent variables. We denote them by a, b, c and d and their arrangement can be seen in eq. (2.27) with a type IV diamond as an example. However, the number of independent variables gets further reduced down to two by the two relations coming from eq. (2.28) with $p = 1, 2$. For type IV diamonds this means for example that

$$c = h^{3,1} - 1 - a - b \tag{2.31}$$

$$d = h^{2,2} - 2b\,, \tag{2.32}$$

picking a and b as the independent variables. Similar relations hold for the other types, so that in total a diamond is fully specified by its Latin numeral, a and b. We therefore introduce the following notation for the Deligne diamonds of singularities in the complex moduli space of Calabi-Yau fourfolds:

$$\mathrm{I}_{a,b} \quad \mathrm{II}_{a,b} \quad \mathrm{III}_{a,b} \quad \mathrm{IV}_{a,b} \quad \mathrm{V}_{a,b} \tag{2.33}$$

Table 2.1 lists the form and the restrictions on a and b of each of these diamonds.

For easier identification of the types, the last column lists the rank of N and its powers and the sign of the eigenvalues of ηN^2 if needed. The ranks were determined by counting the dimensions of the spaces that do not get mapped to zero by the respective operator. Because this method is not able to distinguish type I, II and III, we also looked at the eigenvalues of ηN^l, where η is the matrix corresponding to S, see eq. (1.19). Let us explain how to determine the sign of these eigenvalues. In section 2.4 we will introduce the primitive spaces P_{n+l} which correspond roughly to the Gr_{n+l}. These P_{n+l} are polarized by $S(\cdot, N^l \cdot)$, so from the analog of eq. (2.3) we can deduce the number and sign of the eigenvalues of ηN^l. For $n + l$ odd, these are purely real with alternating sign; for $n + l = 4 + 2$ they can be used to distinguish type III diamonds from type I and II. If $n + l$ even, the eigenvalues are purely imaginary and come in complex conjugate pairs. Therefore they cannot be used for a further distinction. It is not possible to distinguish type I and II with this method, also not with the eigenvalues of just η. It carries no information about N and therefore has the same eigenvalues for all types.

2.3 On the classification of infinite distance points

We can use this classification now for a first result about points at infinite distance in the complex structure moduli space of Calabi-Yau fourfolds. A point P is said to be at infinite distance, if every path leading to it is infinitely long as measured with the Kähler metric $G_{\alpha\bar{\beta}}$, see eq. (1.26). In turn it is said to be at finite distance, if there is at least one path being finitely long in $G_{\alpha\bar{\beta}}$. We first note that any point away from a singular divisor is at finite distance, because the Kähler potential and therefore also the metric is regular in a neighborhood around these points. For the case that the point lies on a

Type	Deligne Diamond	Restrictions	$\mathrm{rank}(N, N^2, N^3, N^4)$
$\mathrm{I}_{a,b}$	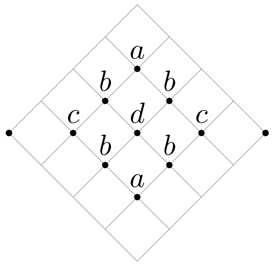	$a, b \geq 0$ $a + b \leq h^{3,1}$ $a + 2b \leq h^{2,2}$ $c = h^{3,1} - a - b$ $d = h^{2,2} - 2b$	$2a + 2b$ a 0 0 ηN^2 has a positive eigenvalues
$\mathrm{II}_{a,b}$	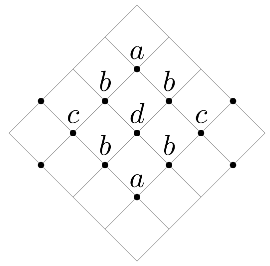	$a, b \geq 0$ $a + b \leq h^{3,1} - 1$ $a + 2b \leq h^{2,2}$ $c = h^{3,1} - 1 - a - b$ $d = h^{2,2} - 2b$	$2a + 2b + 2$ a 0 0 ηN^2 has a positive eigenvalues
$\mathrm{III}_{a,b}$	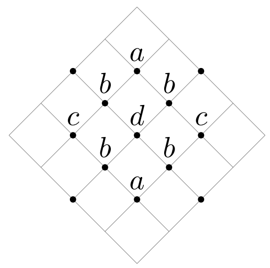	$a, b \geq 0$ $a + b \leq h^{3,1} - 1$ $a + 2b \leq h^{2,2} - 2$ $c = h^{3,1} - a - b$ $d = h^{2,2} - 2 - 2b$	$2a + 2b + 4$ $a + 2$ 0 0 ηN^2 has a positive and 2 negative eigenvalues
$\mathrm{IV}_{a,b}$	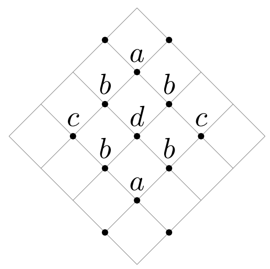	$a \geq 0,\ b \geq 1$ $a + b \leq h^{3,1} - 1$ $a + 2b \leq h^{2,2}$ $c = h^{3,1} - 1 - a - b$ $d = h^{2,2} - 2b$	$2a + 2b + 4$ $a + 4$ 2 0
$\mathrm{V}_{a,b}$	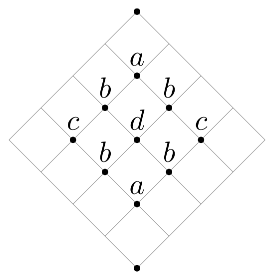	$a \geq 1,\ b \geq 0$ $a + b \leq h^{3,1}$ $a + 2b \leq h^{2,2}$ $c = h^{3,1} - a - b$ $d = h^{2,2} - 2b$	$2a + 2b + 2$ $a + 2$ 2 1

Table 2.1: The five types of singularities in the complex structure moduli space of a Y_4 with Hodge numbers $h^{4,0} = 1$, $h^{3,1}$ and $h^{2,2}$. The different types are distinguished by the form of their Deligne diamond for the limiting mixed Hodge structure that gets assigned to $H^4(Y_4)$ at the singularity. For each type there are two free parameters, a and b, restricted by a system of inequalities. The form and labels of the diamonds are restricted by the properties of eqs. (2.28) to (2.30). The calculation of the ranks and eigenvalues is explained at the end of section 2.2. A graphical notation was used for the diamonds: the label at a dot at (p, q) represents the value of $i^{p,q}$, a dot without label represents the value 1 and no dot represents 0.

singular divisor, i.e. $P \in \Delta$, one has to distinguish two cases. Either, P lies on a single divisor, away from any intersections, i.e. $P \in \Delta_i^\circ$, or P lies on the intersection of two or more divisors, i.e. $P \in \Delta_{i_1 \dots i_k}$. We will discuss both cases in turn.

For P lying on a single divisor Δ_i°, it was shown by Wang [21] that P is at finite distance if $NF^4(\Delta_i^\circ) = 0$. Because of the location of $F^4(\Delta_i^\circ)$ in the Deligne splitting (see fig. 2.2) and the fact that $NI^{p,q} \subset I^{p-1,q-1}$ we conclude that only points on divisors of type I lie at finite distance:

$$\begin{aligned} P \text{ at finite distance} &\iff \Delta_i^\circ \text{ of type I} \\ P \text{ at infinite distance} &\iff \Delta_i^\circ \text{ of type II, III, IV or V} \,. \end{aligned} \tag{2.34}$$

In the second case of P lying at an intersection of divisors $\Delta_{i_1 \dots i_k}$ the situation becomes more involved. Because of the multi-parameter degeneration, the path dependence of the distance can make a qualitative difference and it is more difficult to show infinite length for all paths. Nevertheless Grimm, Li and Palti [12] give a short argument for the following result:

$$\begin{aligned} P \text{ at finite distance} &\Longleftarrow \Delta_{i_1 \dots i_k} \text{ of type I} \\ P \text{ at infinite distance} &\Longrightarrow \Delta_{i_1 \dots i_k} \text{ of type II, III, IV or V} \,. \end{aligned} \tag{2.35}$$

Further, Wang [22] conjectured that these statements are actually equivalences, similar to eq. (2.34), which we will assume in the following.

2.4 Singularity enhancements and their classification

Consider a Calabi-Yau with multiple moduli and let us go to a singular locus in moduli space, such that the Calabi-Yau is degenerate. It may happen that it is now possible to make the manifold even more degenerate by tuning another moduli. This happens when two singular loci, Δ_1 and Δ_2, are crossing; fig. 2.4 visualizes this. If we move from Δ_1° to the intersection Δ_{12}°, the type of the singularity, as classified by their diamonds from table 2.1, can change as well. This so called *enhancement* of the singularity type will be denoted by $A_1 \to A_{12}$, where A_1 and A_{12} is the type of the singularity at Δ_1° and Δ_{12}° respectively. For these enhancements there are consistency conditions for the mixed Hodge structures on the divisors [20] and it turns out that there are constraints on the types of singularities that can be part of an enhancement. To tackle the derivation of these constraints in the following we will first introduce the notion of primitive spaces. We are then able to transform the problem again into one of combinatorics. The results are listed in table 2.2. Our exposition follows [18].

The primitive spaces of a mixed Hodge structure (F, N) are the subspaces of the $I^{p,q}$ that are not generated by $NI^{p+1,q+1}$ (remember $NI^{p+1,q+1} \subset I^{p,q}$, see eq. (2.23)). They are defined by

$$P^{p,q} = \ker(N^{p+q-n+1} \colon I^{p,q} \to I^{n-q-1,n-p-1}) \quad \text{for } p+q \geq n \,. \tag{2.36}$$

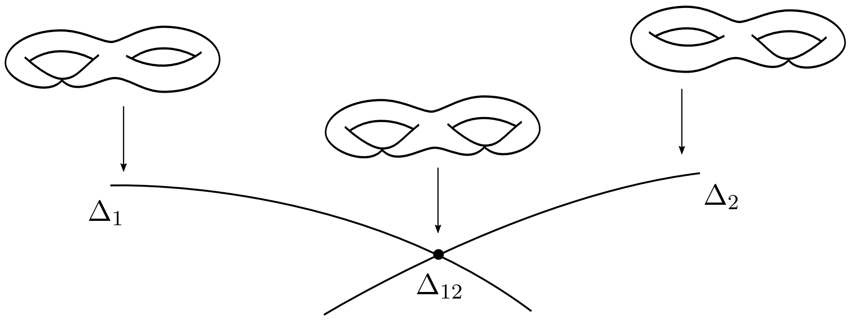

Figure 2.4: Example degeneration of a double-torus at individual divisors in moduli space and how it gets worse at their intersection. A similar worsening of the degeneration happens to Calabi-Yau manifolds at their intersecting divisors.

The $I^{p,q}$ of the Deligne splitting can now be expressed in terms of the primitive spaces $P^{p,q}$ and their images under N. The splitting of H^n in eq. (2.10) then takes the form

$$\begin{array}{ccccccccc}
 & & & & P^{4,4} & & & & \\
 & & & P^{4,3} & & P^{3,4} & & & \\
 & & P^{4,2} & & P^{3,3} \oplus NP^{4,4} & & P^{2,4} & & \\
 & P^{4,1} & & P^{3,2} \oplus NP^{4,3} & & P^{2,3} \oplus NP^{3,4} & & P^{1,4} & \\
P^{4,0} & & P^{3,1} \oplus NP^{4,2} & & P^{2,2} \oplus NP^{3,3} \oplus N^2P^{4,4} & & P^{1,3} \oplus NP^{2,4} & & P^{0,4} . \\
 & NP^{4,1} & & NP^{3,2} \oplus N^2P^{4,3} & & NP^{2,3} \oplus N^2P^{3,4} & & NP^{1,4} & \\
 & & N^2P^{4,2} & & N^2P^{3,3} \oplus N^3P^{4,4} & & N^2P^{2,4} & & \\
 & & & N^3P^{4,3} & & N^3P^{3,4} & & & \\
 & & & & N^4P^{4,4} & & & &
\end{array} \tag{2.37}$$

Analogous to the Deligne diamond, listing the dimensions of the $I^{p,q}$ (see eq. (2.26)), we can also give a primitive diamond, listing the dimensions of the $P^{p,q}$. With $j^{p,q} \coloneqq \dim_{\mathbb{C}} P^{p,q}$ this becomes

$$\begin{array}{ccccccccc}
 & & & & j^{4,4} & & & & \\
 & & & j^{4,3} & & j^{3,4} & & & \\
 & & j^{4,2} & & j^{3,3} & & j^{2,4} & & \\
 & j^{4,1} & & j^{3,2} & & j^{2,3} & & j^{1,4} & \\
j^{4,0} & & j^{3,1} & & j^{2,2} & & j^{1,3} & & j^{0,4} \\
 & 0 & & 0 & & 0 & & 0 & \\
 & & 0 & & 0 & & 0 & & \\
 & & & 0 & & 0 & & & \\
 & & & & 0 & & & &
\end{array}
=
\begin{array}{ccccccccc}
 & & & & \bullet\, j^{4,4} & & & & \\
 & & & \bullet\, j^{4,3} & & \bullet\, j^{3,4} & & & \\
 & & \bullet\, j^{4,2} & & \bullet\, j^{3,3} & & \bullet\, j^{2,4} & & \\
 & \bullet\, j^{4,1} & & \bullet\, j^{3,2} & & \bullet\, j^{2,3} & & \bullet\, j^{1,4} & \\
\bullet\, j^{4,0} & & \bullet\, j^{3,1} & & \bullet\, j^{2,2} & & \bullet\, j^{1,3} & & \bullet\, j^{0,4}
\end{array} \tag{2.38}$$

We further combine the $P^{p,q}$ on the same horizontal line into *horizontal primitive spaces* analogous to the Gr_l:

$$P_{n+l} \coloneqq \bigoplus_{p+q=n+l} P^{p,q} \,. \tag{2.39}$$

And with this, the decomposition eq. (2.37) of the total space H^n can be compactly written as

$$H^n = \bigoplus_{l=0}^{n} \bigoplus_{a=0}^{l} N^a P_{n+l} \, . \tag{2.40}$$

The horizontal primitive spaces are important because the primitive spaces determine a Hodge structure on them: $P^{p,q}$ gives a Hodge structure of weight $n+l$ on P_{n+l}. The Hodge numbers are $j^{p,q}$ and it is polarized by $S_l \coloneqq S(\cdot, N^l \cdot)$ instead of just $S(\cdot,\cdot)$, see eqs. (2.2) and (2.3).

We are coming now to the main step for the enhancement procedure, where we are going to use the N_i^- of the commuting $\mathfrak{sl}_2$-triplets. Because N_2^- leaves the horizontal spaces Gr_{n+l} (by construction) invariant and commutes with N_1^- it also leaves the primitive horizontal spaces P_{n+l} invariant. This means that something similar to the original situation where N left H^n invariant happens. There, as we approached the divisor Δ_1, N turned the Hodge structure on H^n into a mixed Hodge structure. In the same spirit, as we approach the intersection of divisors Δ_{12}, N_2^- turns the Hodge structures on P_{n+l} into mixed Hodge structures. As we add up these mixed Hodge structures according to eq. (2.40) we get the total limiting mixed Hodge structure assigned to Δ_{12}. Turning this argument around, this means that an enhancement $A_1 \to A_{12}$ is possible, if there exist mixed Hodge structures for the horizontal primitive spaces P_{n+l} of the mixed Hodge structure of type A_1 (assigned to Δ_1) that, when added up, give the mixed Hodge structure of type A_{12} (assigned to Δ_{12}).

The last step is now to make this condition more manageable and translate it to the level of Deligne diamonds. For this denote the diamonds of A_1 and A_{12} by $\Diamond_1$ and $\Diamond_{12}$ respectively and the diamonds for the P_{n+l} by $\Diamond'_{n+l}$. With this eq. (2.40) translates into

$$\Diamond_{12} = \sum_{l=0}^{n} \sum_{a=0}^{l} \Diamond'_{n+l}[a] \tag{2.41}$$

where $\Diamond[a]$ is the diamond $\Diamond$ offset by a steps downwards. This means an enhancement is possible if there are diamonds $\Diamond'_{n+l}$ for the mixed Hodge structures on P_{n+l} such that their sum according to the above equation gives $\Diamond_{12}$.

The possible enhancements according to this condition are listed in table 2.2. To get a better understanding of how to derive these we will however first discuss an example, though.

Example: the enhancement $\mathbf{II}_{a,b} \to \mathbf{IV}_{\tilde{a},\tilde{b}}$. For $n=4$, we will look at the enhancement $\mathrm{II}_{a,b} \to \mathrm{IV}_{\tilde{a},\tilde{b}}$ with diamonds from table 2.1. The primitive diamond of type $\mathrm{II}_{a,b}$ is given by

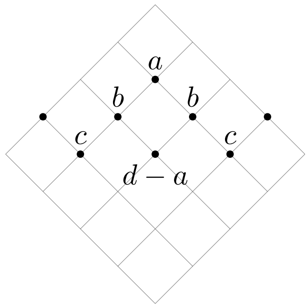

(2.42)

This means we must find three diamonds (restricted through eqs. (2.28) to (2.30) by the Hodge numbers $\mathbf{h}'_{4+l}$ of the horizontal primitive spaces P_{4+l})

- $\Diamond'_4$ with Hodge numbers $\mathbf{h}'_4 = (0, c, d-a, c, 0)$
- $\Diamond'_{4+1}$ with Hodge numbers $\mathbf{h}'_{4+1} = (0, 1, b, b, 1, 0)$
- $\Diamond'_{4+2}$ with Hodge numbers $\mathbf{h}'_{4+2} = (0, 0, 0, a, 0, 0, 0)$

such that their sum gives

$$\Diamond_{12} \overset{!}{=} \Diamond'_4 + \Diamond'_{4+1} + \Diamond'_{4+1}[1] + \Diamond'_{4+2} + \Diamond'_{4+2}[1] + \Diamond'_{4+2}[2]\,. \tag{2.43}$$

The possible diamonds for the $\Diamond'_{4+l}$ can be found (after ignoring the surrounding zeros) in [12, 20]. The full enhancement with the right type of diamonds is displayed in fig. 2.5. The choice of diamond for $\Diamond'_4$ leaves us with the free variables a', b', c' and d'. Through the properties of Deligne diamonds eqs. (2.28) to (2.30), these are related and constrained by

$$0 \le a' \qquad\qquad 0 \le c' = c - a' - b' \tag{2.44}$$
$$0 \le b' \qquad\qquad a' \le d' = d - a - 2b'\,. \tag{2.45}$$

For $\Diamond'_{4+1}$ we have the variable e' with constraints

$$0 \le e' \qquad\qquad 1 \le b - 1 - e'\,. \tag{2.46}$$

In total, with the expressions for c and d for type $\mathrm{II}_{a,b}$ from table 2.1 filled in, we are left with the free variables a', b' and e' constrained by

$$0 \le a' \qquad\qquad 0 \le h^{3,1} - 1 - a - b - a' - b' \tag{2.47}$$
$$0 \le b' \qquad\qquad 0 \le h^{2,2} - a - 2b - a' - 2b' \tag{2.48}$$
$$0 \le e' \le b - 2\,. \tag{2.49}$$

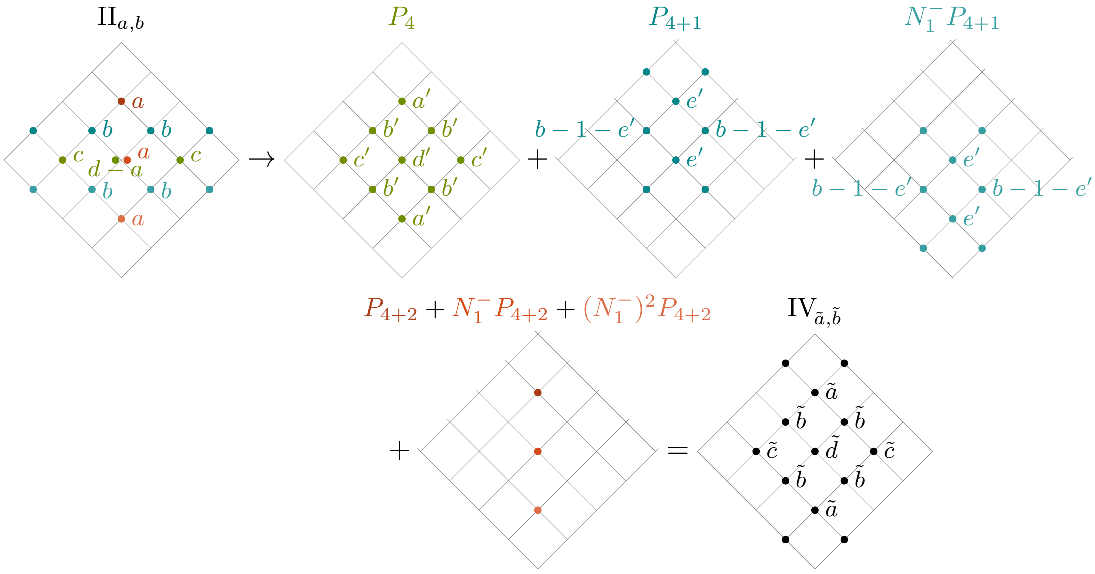

Figure 2.5: The enhancement $\mathrm{II}_{a,b} \to \mathrm{IV}_{\tilde{a},\tilde{b}}$ with the Deligne diamonds for the horizontal primitive space P_{4+l} allowing for it. The colors signal which diamonds are associated to the respective horizontal primitive spaces of the type $\mathrm{II}_{a,b}$ mixed Hodge structure. A more detailed explanation how to assign these can be found in the text.

Adding now all diamonds according to eq. (2.43) together and equating them with $\Diamond_{12}$ gives the following condition for the enhancement:

$$\tilde{a} \overset{!}{=} a + a' + e' \tag{2.50}$$

$$\tilde{b} \overset{!}{=} b + b' - e' \tag{2.51}$$

$$\tilde{c} = h^{3,1} - 1 - \tilde{a} - \tilde{b} \overset{!}{=} h^{3,1} - 1 - a - b - a' - b' \tag{2.52}$$

$$\tilde{d} = h^{2,2} - 2\tilde{b} \overset{!}{=} h^{2,2} - 2b - 2b' + 2e' \,. \tag{2.53}$$

In the last two lines the expressions for $\tilde{c}$ and $\tilde{d}$ for type $\mathrm{IV}_{\tilde{a},\tilde{b}}$ diamonds from table 2.1 were used. With this, it is easy to see that these last two equations are trivially fulfilled by the first two equations for $\tilde{a}$ and $\tilde{b}$. The question is now, is it always possible to pick a', b' and e' such that these first two are fulfilled? Using a bit of algebra or the more systematic Fourier-Motzkin elimination we can show that this is only possible if a, b, $\tilde{a}$ and $\tilde{b}$ satisfy

$$a \leq \tilde{a} \qquad 2 \leq b \qquad 2 \leq \tilde{b} \tag{2.54}$$

$$a + b \leq \tilde{a} + \tilde{b} \leq h^{2,2} - b \tag{2.55}$$

in addition to the conditions for a and b for type II and for $\tilde{a}$ and $\tilde{b}$ for type IV from table 2.1.

The same procedure can be followed for all combinations of initial and enhanced type; the resulting allowed enhancements and their respective constraints can be found in table 2.2. The main feature to note there is that for enhancements with the second type smaller than the first type, it is not possible to pick suiting diamonds $\Diamond'_{4+l}$ and therefore no enhancement is possible. For the other cases we find similar constraints as for the example discussed.

Initial Type	Enhanced Type	Constraints
$\mathrm{I}_{a,b}$	$\mathrm{I}_{\tilde{a},\tilde{b}}$	$a \leq \tilde{a}$ $a+b \leq \tilde{a}+\tilde{b} \leq h^{2,2}-b$
	$\mathrm{II}_{\tilde{a},\tilde{b}}$	$a \leq \tilde{a}$ $a+b \leq \tilde{a}+\tilde{b} \leq h^{2,2}-b$
	$\mathrm{III}_{\tilde{a},\tilde{b}}$	$a \leq \tilde{a}$ $a+b \leq \tilde{a}+\tilde{b} \leq h^{2,2}-b-2$
	$\mathrm{IV}_{\tilde{a},\tilde{b}}$	$a \leq \tilde{a}$ $a+b+1 \leq \tilde{a}+\tilde{b} \leq h^{2,2}-b-2$
	$\mathrm{V}_{\tilde{a},\tilde{b}}$	$a+1 \leq \tilde{a}$ $a+b+1 \leq \tilde{a}+\tilde{b} \leq h^{2,2}-b$
$\mathrm{II}_{a,b}$	$\mathrm{II}_{\tilde{a},\tilde{b}}$	$a \leq \tilde{a}$ $a+b \leq \tilde{a}+\tilde{b} \leq h^{2,2}-b$
	$\mathrm{III}_{\tilde{a},\tilde{b}}$	$a \leq \tilde{a} \quad 1 \leq b$ $a+b-1 \leq \tilde{a}+\tilde{b} \leq h^{2,2}-b-1$ $\tilde{a}+\tilde{b} \leq h^{3,1}-2$
	$\mathrm{IV}_{\tilde{a},\tilde{b}}$	$a \leq \tilde{a} \quad 2 \leq b,\tilde{b}$ $a+b \leq \tilde{a}+\tilde{b} \leq h^{2,2}-b$
	$\mathrm{V}_{\tilde{a},\tilde{b}}$	$a+2 \leq \tilde{a} \quad 1 \leq b$ $a+b+1 \leq \tilde{a}+\tilde{b} \leq h^{2,2}-b+1$
$\mathrm{III}_{a,b}$	$\mathrm{III}_{\tilde{a},\tilde{b}}$	$a \leq \tilde{a}$ $a+b \leq \tilde{a}+\tilde{b} \leq h^{2,2}-b-2$
	$\mathrm{IV}_{\tilde{a},\tilde{b}}$	$a-2 \leq \tilde{a} \quad 2 \leq a,\tilde{b}$ $a+b \leq \tilde{a}+\tilde{b} \leq h^{2,2}-b-2$
	$\mathrm{V}_{\tilde{a},\tilde{b}}$	$a+2 \leq \tilde{a} \quad 1 \leq a$ $a+b+1 \leq \tilde{a}+\tilde{b} \leq h^{2,2}-b-1$ $\tilde{a}+2\tilde{b} \leq h^{2,2}-1$
$\mathrm{IV}_{a,b}$	$\mathrm{IV}_{\tilde{a},\tilde{b}}$	$a \leq \tilde{a}$ $a+b \leq \tilde{a}+\tilde{b} \leq h^{2,2}-b$
	$\mathrm{V}_{\tilde{a},\tilde{b}}$	$a+2 \leq \tilde{a}$ $a+b+1 \leq \tilde{a}+\tilde{b} \leq h^{2,2}-b+1$
$\mathrm{V}_{a,b}$	$\mathrm{V}_{\tilde{a},\tilde{b}}$	$a \leq \tilde{a}$ $a+b \leq \tilde{a}+\tilde{b} \leq h^{2,2}-b$

Table 2.2: Allowed enhancements between the singularities in the complex moduli space of a Y_4 with Hodge numbers $h^{4,0}=1$, $h^{3,1}$ and $h^{2,2}$ listed in table 2.1. An enhancement occurs when we make an already degenerate Y_4 even more degenerate. See the text for a mathematical definition and fig. 2.4 for an intuitive picture. The third column lists a system of inequalities that needs to be fulfilled by a, b, $\tilde{a}$ and $\tilde{b}$ besides the conditions in table 2.1. The allowed enhancements were derived by imposing consistency conditions that are explained in detail in section 2.4.

3 Infinite and massless towers of states on singular Calabi-Yau fourfolds

3.1 Definition of the general charge orbit

In the following discussion, we try to find the, by the Swampland Distance Conjecture predicted, tower of states that becomes infinite and massless as we approach a singular point P at infinite distance. According to section 2.3 we expect this to be only possible for points of type II to V.

We consider such a P that lies in a neighborhood $\mathcal{E}$ of $n_{\mathcal{E}}$ crossing divisors, i.e. $\mathcal{E}$ is a neighborhood of $\Delta_{(n_{\mathcal{E}})}$. In contrast, n_P denotes the number of divisors that cross at P itself. With a suiting labeling of the divisors we therefore have $P \in \Delta^{\circ}_{(n_P)} \subset \mathcal{E}$.

This gives us an enhancement chain of the different types of the divisors in $\mathcal{E}$. If $A_{(i)}$ is the singularity type of $\Delta^{\circ}_{(i)}$, then we denote this enhancement chain by

$$A_{(1)} \to A_{(2)} \to \cdots \to \boldsymbol{A_{(n_P)}} \to \cdots \to A_{(n_{\mathcal{E}})} \ , \tag{3.1}$$

where we indicated the location of P with boldface. Of course, each of these enhancements has to be allowed according to table 2.2. We fix the labels of the first $n_P - 1$ divisors in such a way that the path of approach we are interested in, fulfills the requirements of the growth theorem; the details of this will be explained below.

As the main character in this analysis we have D4-branes wrapping the internal fourfold. In a single divisor scenario it was argued in [6] that on threefolds these are BPS states. We assume that this property carries over to the multi divisor case and fourfolds. The BPS property allows us to calculate the mass of the states in terms of their central charge, as will be explained in a moment.

Following the construction of [12], we define now a tower of such BPS states, where each state is expressed as an element in H^4 representing the Poincaré dual of the D4-brane. We call this tower *charge orbit*

$$\mathbf{Q}(\mathbf{q}_0|\{m_i\}) = \exp\left(\sum_i^{n_{\mathcal{E}}} m_i N_i^-\right)\mathbf{q}_0 \tag{3.2}$$

and it is derived from a seed charge $\mathbf{q}_0 \in H^4$ by acting with the monodromy logarithms N_i^- multiplied by some $m_i \in \mathbb{Z}$. Here the N_i^- are part of commuting $\mathfrak{sl}_2$-triplets that can be constructed from the N_i; again we refer to [12] for a review. The construction can be seen as switching to a special basis that has a number of nice properties. These will be explained later. How to pick the seed charge $\mathbf{q}_0$ will be the content of the major part of this chapter.

When does $\mathbf{Q}$ fulfill now the conditions of the SDC of being infinite and massless? The first condition holds if $N_i^-\mathbf{q}_0 \neq 0$, for some i, as can easily be seen by noting that the N_i^- are nilpotent. This means that their eigenvectors have all zero eigenvalue. So our requirement means that $\mathbf{q}_0$ is not an eigenvector and therefore already the first term of the expanded exponential, $\left(1 + m_i N_i^-\right)\mathbf{q}_0$, gives different states for each m_i. It follows that the orbit is infinite.

When is it massless? To answer this we have to do some calculations first. As stated earlier, the mass of a BPS state is given in terms of its central charge. Explicitly it is $M(\mathbf{Q}) = |Z(\mathbf{Q})|$. The central charge for a D4-brane BPS state is in turn given by

$$Z(\mathbf{Q}) = \mathrm{e}^{\frac{K}{2}} \int_{Y_4} \mathbf{Q} \wedge \Omega \,, \tag{3.3}$$

where $K = -\ln \|\Omega\|^2$ is the Kähler potential given by eq. (1.27) and Ω is the holomorphic Calabi-Yau $(4,0)$-form. Because for such a $(4,0)$-form we have $\star\overline{\Omega} = \Omega$, we can rewrite this with the Hodge inner product from eq. (1.20) and insert K:

$$Z(\mathbf{Q}) = \frac{\langle \mathbf{Q} | \Omega \rangle}{\|\Omega\|} \,. \tag{3.4}$$

For the mass of $\mathbf{Q}$ follows with help of the Cauchy-Schwarz inequality

$$M(\mathbf{Q}) = |Z(\mathbf{Q})| = \frac{|\langle \mathbf{Q} | \Omega \rangle|}{\|\Omega\|} \leq \frac{\|\mathbf{Q}\| \|\Omega\|}{\|\Omega\|} = \|\mathbf{Q}\| \,. \tag{3.5}$$

We see that if $\|\mathbf{Q}\|$ goes to zero, M goes to zero as well. As will become clear in section 3.5, we can replace $\|\mathbf{Q}\|$ with $\|\mathbf{q}_0\|$ in this statement with out altering its validity.

In summary we have two properties that the seed charge $\mathbf{q}_0$ needs to satisfy for the charge orbit $\mathbf{Q}(\mathbf{q}_0|\{m_i\})$ to be infinite and massless. Firstly, it needs to fulfill $N_i^-\mathbf{q}_0 \neq 0$ for at least one i and secondly, $\|\mathbf{q}_0\|$ needs to go to zero as we approach the singular point. Candidates fulfilling these two properties can be easily identified using the technology of mixed Hodge structures defined in the previous chapter and a detailed explanation of how to do this will follow. We will in turn discuss the cases where $n_\mathcal{E}$ is 1, 2 or an arbitrary number.

3.2 Analysis for a one divisor neighborhood

In the case of only one divisor, i.e. $n_\mathcal{E} = 1$, we simply have $N_1^- \equiv N_1$. The charge orbit is therefore

$$\mathbf{Q}(\mathbf{q}_0; m_1) = \exp(m_1 N_1)\mathbf{q}_0 \,. \tag{3.6}$$

We further know that N_1 acts like $N_1 I^{p,q} \subset I^{p-1,q-1}$; a graphical representation of this can be seen in fig. 3.1. With this we can use the Deligne diamonds to easily read off which subspaces $I^{p,q}$ have elements $\mathbf{q}_0$ fulfilling $N_1\mathbf{q}_0 \neq 0$. [1]

[1] Note that $\mathbf{q}_0$ has to be picked from a fitting primitive part of $I^{p,q}$ (see eq. (2.37)) to ensure that it actually gets mapped to a non-zero value. One way to guarantee this, is to express $\mathbf{q}_0$ in terms of $\tilde{\mathbf{a}}_0^{(n_\mathcal{E})}$.

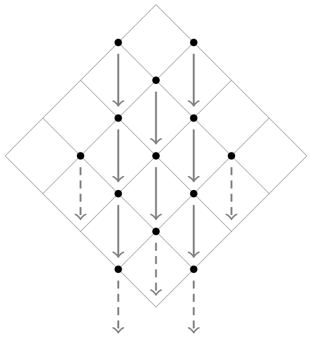

Figure 3.1: Graphical representation of the action $N_1 I^{p,q} \subset I^{p-1,q-1}$ of the monodromy logarithm N_1 on the spaces $I^{p,q}$ of a type $\mathrm{IV}_{a,b}$ mixed Hodge structure. As explained in section 2.2, a dot denotes a space of dimension one or greater (labels are omitted). No dot denotes a null space. The arrows indicate the action of N_1. The solid arrows represent faithful mappings and dotted arrows zero mappings.

To estimate the mass of the states we use the growth theorem for flat sections around a singularity from [19]: if we're given a vector $\mathbf{v} \in Gr_{4+l_1}$ then the norm of the by parallel transport derived section behaves to leading order like

$$\|\mathbf{v}\|^2 \sim y_1^{l_1} , \tag{3.7}$$

for $y_1 > \lambda$, where $y_1 = \mathrm{Im}\, t_1$ and λ is a sufficiently large constant. The singular point lies at $t_1 \to +\mathrm{i}\infty$ and therefore $y_1 \to \infty$.

Because $M(\mathbf{Q}) \leq \|\mathbf{q}_0\|$ we want $\mathbf{q}_0 \to 0$ to guarantee that the mass $M(\mathbf{Q})$ goes to zero as well. From this we deduce that we need $\mathbf{q}_0 \in Gr_{4+l_1}$ with $l_1 < 0$.

We can now look at the Hodge diamonds of the different singularity types in table 2.1 and try to identify a $\mathbf{q}_0$ fulfilling the two conditions for each of them. As seen in fig. 3.2 it is only possible for type IV and V to find a $I^{p,q}$ that lies below the diagonal and is not mapped to zero by N_1. The elements of its subspace that don't get mapped to zero are generated by $N_1^2\mathbf{a}_0$ for type IV and by $N_1^3\mathbf{a}_0$ for type V. Remember $\mathbf{a}_0$ is the vector spanning F^4_Δ, see eq. (2.16), which in turn is composed of the top-left most spaces in the Deligne splitting, see fig. 2.2. It is thus natural to pick

$$\mathbf{q}_0 = N_1^2\mathbf{a}_0 \quad \text{for type } \mathrm{IV}_{a,b} \, , \tag{3.8}$$

$$\mathbf{q}_0 = N_1^3\mathbf{a}_0 \quad \text{for type } \mathrm{V}_{a,b} \, . \tag{3.9}$$

3.3 Analysis for a two divisor neighborhood

We turn now to the case $n_\mathcal{E} = 2$, i.e. the singular point P is located in a neighborhood $\mathcal{E}$ of two intersecting divisors Δ_1 and Δ_2. If P lies away from the intersection, we pick the indices of the two divisors such that $P \in \Delta_1^\circ$. Denoting the singularity type of $\Delta_1^\circ \equiv \Delta_{(1)}^\circ$ with $A_{(1)}$ and the type of $\Delta_{12} \equiv \Delta_{(2)}$ with $A_{(2)}$, then the enhancement pattern is given

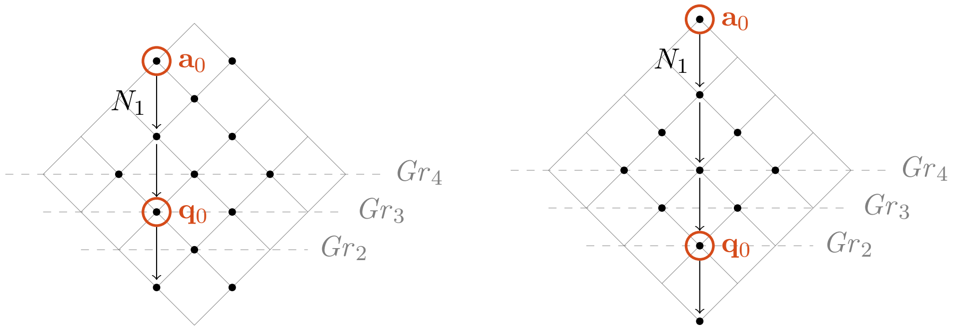

Figure 3.2: Hodge diamonds for type IV and V singularities with the location of $\mathbf{q}_0$ and $\mathbf{a}_0$ indicated. $\mathbf{q}_0$ lies below the diagonal and therefore fulfills $\mathbf{q}_0 \in Gr_{4+l_1}$ with $l_1 < 0$. Further they get mapped to a value in a non-zero vector space by N_1, as indicated by the arrows. This shows the existence of an infinite charge orbit for type IV and V singularities; for type I, II and III such a choice does not exist.

by $\boldsymbol{A_{(1)}} \to A_{(2)}$. In case P lies on the intersection, i.e. $P \in \Delta_{(2)}$, we pick the ordering of the indices of Δ_1 and Δ_2 such that the path on which we are approaching P lies in the growth sector eq. (3.13) that is part of the growth theorem (we will explain this in a second). The enhancement pattern is then given by $A_{(1)} \to \boldsymbol{A_{(2)}}$. Both situations are displayed in fig. 3.3.

The charge orbit, we are trying to identify, is now defined by

$$\mathbf{Q}(\mathbf{q}_0; m_1, m_2) = \exp\bigl(m_1 N_1^- + m_2 N_2^-\bigr)\mathbf{q}_0\,. \tag{3.10}$$

Here, the N_i^- are part of commuting $\mathfrak{sl}_2$-triplets that can be constructed from the N_i; again we refer to [12] for a review.

The important point is how they act on the spaces $I^{p,q}$ across an enhancement $A_{(1)} \to A_{(2)}$. As exemplified in fig. 3.4, they have a well-defined mapping behavior respecting the decomposition in primitive spaces and their diamonds. N_1^- maps between the primitive spaces $P^{(1)}_{4+l}$ of $A_{(1)}$, before as well as after the enhancement. Because it commutes with N_2^- it does not alter the structure of the mixed Hodge structures induced by N_2^- after the enhancement. In turn, because N_2^- leaves the primitive spaces $P^{(1)}_{4+l}$ invariant, it maps only within these after the enhancement. This well-defined mapping behavior gives us therefore an easy way of reading of the infiniteness condition from the diagrams of the enhancement:

$$N_1^- \mathbf{q}_0 \neq 0 \quad \text{or} \quad N_2^- \mathbf{q}_0 \neq 0\,. \tag{3.11}$$

For the masslessness condition $\|\mathbf{q}_0\| \to 0$ we use again the growth theorem. In case that P lies on the intersection $\Delta_{(2)}$ we need to use the two variable version, which, however, features a path dependence. The theorem states that a vector $\mathbf{v} \in Gr^{(1)}_{4+l_1} \cap Gr^{(2)}_{4+l_2}$ (where $Gr^{(i)}_{4+l_i}$ are the graded spaces eq. (2.25) of $A_{(i)}$) has the leading order growth

$$\|\mathbf{v}\|^2 \sim \left(\frac{y_1}{y_2}\right)^{l_1} (y_2)^{l_2} \tag{3.12}$$

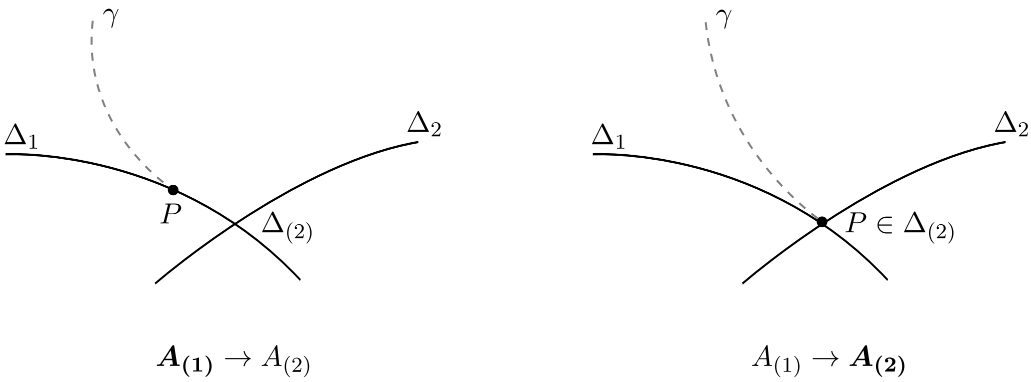

Figure 3.3: Moduli space with two intersecting divisors. The singular point P can either lie away or on the intersection $\Delta_{(2)}$; its location is indicated by boldface in the enhancement chain. $A_{(2)}$ denotes the singularity type of the intersection. The dotted line gives the path of approach γ; the numbering of divisors Δ_1 and Δ_2 is chosen such that γ lies within the growth sector of eq. (3.13).

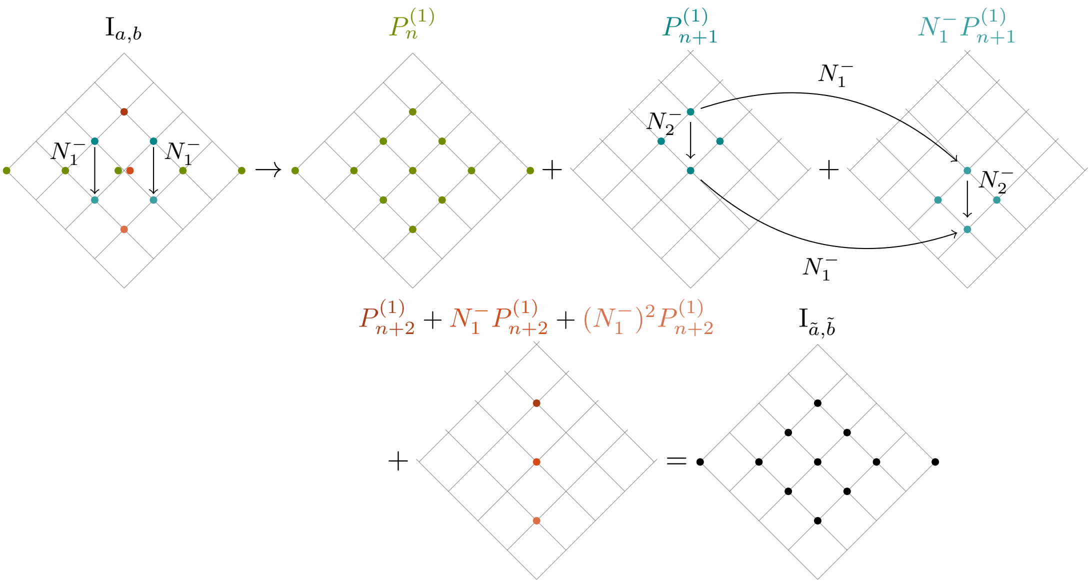

Figure 3.4: The example enhancement $\mathrm{I}_{a,b} \to \mathrm{I}_{\tilde{a},\tilde{b}}$ with the subdiamonds induced by the primitive space $P_{4+l}^{(1)}$. The actions of N_1^- and N_2^- across an enhancement are indicated by arrows. N_1^- maps $I_{(1)}^{p,q}$ to $I_{(1)}^{p-1,q-1}$ in the splitting at $\Delta_{(1)}^\circ$ before and after the enhancement. On the other hand N_2^- maps $I_{(2)}^{p,q}$ to $I_{(2)}^{p-1,q-1}$ in the splitting at $\Delta_{(2)}^\circ$ after the enhancement, staying within the subdiamonds induced by the primitive spaces. The particular definition of the N_i^- ensures this well defined behavior.

for a path in the growth sector

$$\frac{y_1}{y_2}\,, y_2 > \lambda\,, \quad x_1, x_2 < \delta\,, \tag{3.13}$$

for some constants λ and δ. We pick the ordering of the indices of Δ_1 and Δ_2 such that the path on which we are approaching P lies within this sector. That means we eventually have to exchange the indices 1 and 2.

Because of the bound $\frac{y_1}{y_2} > \lambda$ the condition for $\|\mathbf{q}_0\| \to 0$ and therefore masslessness as $y_i \to \infty$ (within the growth sector) is for the two variable case $A_{(1)} \to \boldsymbol{A_{(2)}}$

$$l_1 \leq 0 \quad \text{and} \quad l_2 < 0\,. \tag{3.14}$$

For the one variable case $\boldsymbol{A_{(1)}} \to A_{(2)}$ the condition is the same as in the previous section:

$$l_1 < 0\,. \tag{3.15}$$

We will now look at a few examples of divisor structures and enhancements to demonstrate how we determine the existence of a suitable seed charge $\mathbf{q}_0$ fulfilling the infiniteness and masslessness condition.

The enhancement $\mathrm{II}_{a,b} \to \mathrm{IV}_{\tilde{a},\tilde{b}}$

The Hodge diamond of type II singularities splits into primitive spaces as indicated on the left side in fig. 3.5. On each of these spaces N_2^- induces a new mixed Hodge structure, whose Hodge diamonds are depicted on the right side of the arrow. As describes earlier, an enhancement is possible if the diamonds of these mixed Hodge structures give, when added together, the target type IV diamond. In the diamonds after the enhancement we identified and marked a seed charge $\mathbf{q}_0$ fulfilling the properties eqs. (3.11), (3.14) and (3.15).

- The requirement for infiniteness eq. (3.11) can be easily checked by noting how the two monodromy logarithms act: N_1^- maps between the splittings of associated primitive spaces; N_2^- maps within the splitting of each individual primitive space. We see that $\mathbf{q}_0$ gets mapped to a non-zero value by N_2^-.
- The two criteria for masslessness eqs. (3.14) and (3.15) can be translated into: For the enhancement pattern $A_{(1)} \to \boldsymbol{A_{(2)}}$ the seed charge must be on or below the diagonal on the left hand side and strictly below the diagonal on the right hand side of the enhancement. For the pattern $\boldsymbol{A_{(1)}} \to A_{(2)}$ it must be strictly below the diagonal on the left hand side of the enhancement. The location on the right hand side does not matter. We see that our $\mathbf{q}_0$ fulfills this condition for both cases.

Therefore, for both cases, $\boldsymbol{A_{(1)}} \to A_{(2)}$ and $A_{(1)} \to \boldsymbol{A_{(2)}}$, the marked $\mathbf{q}_0$ in fig. 3.5 indeed generates an infinite and massless charge orbit.

To ensure the first condition actually holds, we want to express $\mathbf{q}_0$ through $\mathbf{a}_0$ again. However, because we were working in the $\mathfrak{sl}_2$-triplet basis, we have to use $\tilde{\mathbf{a}}_0^{(2)}$, which

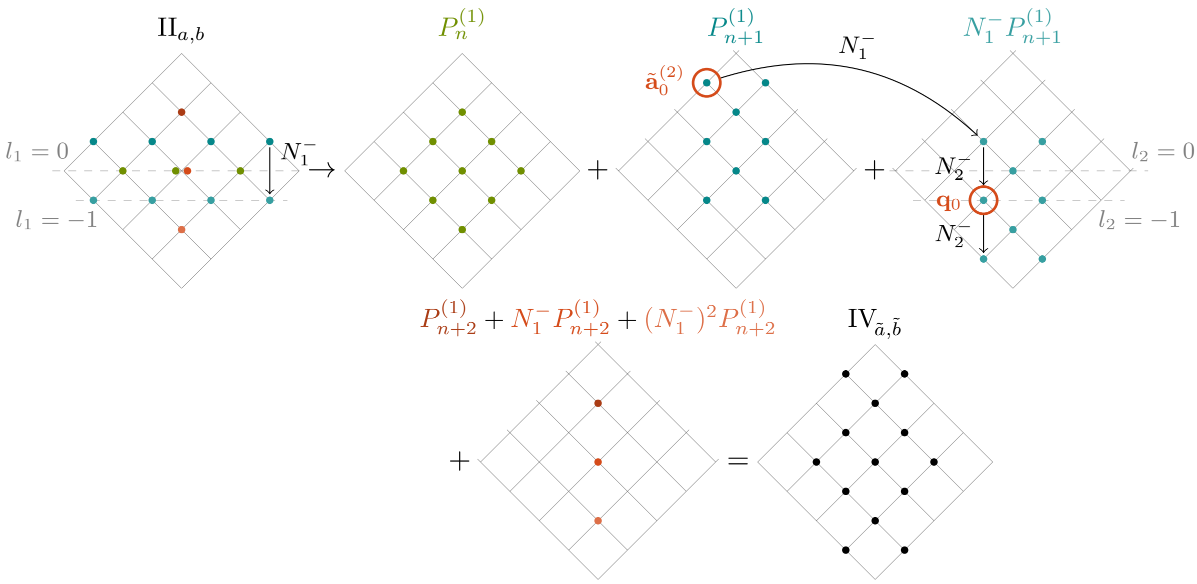

Figure 3.5: Hodge diamonds of a type II singularity and its primitive spaces, enhancing to a type IV singularity. The primitive spaces and their by N_2^- induced mixed Hodge structures are distinguished by color. See section 2.4 for a detailed explanation. The location of the seed charge $\mathbf{q}_0$ for the charge orbit is marked. As indicated, N_2^- sends it to a non-zero space; the charge orbit is therefore infinite. Further the location in the diamonds before and after the enhancement gives $l_1 = -1$ and $l_2 = -1$, which, according to eq. (3.14), makes the charge orbit massless. It is further indicated how to retrieve $\mathbf{q}_0$ from $\tilde{\mathbf{a}}_0^{(2)}$.

is $\mathbf{a}_0$ expressed in this basis. It spans the (one-dimensional) top-left-most space on the enhanced side and $\mathbf{q}_0$ can be written as

$$\mathbf{q}_0 = N_2^- N_1^- \tilde{\mathbf{a}}_0^{(2)} \,. \tag{3.16}$$

3.4 Analysis for an arbitrary number of divisors

The singular point P is now assumed to be on the intersection of n_P singular divisors $P \in \Delta^\circ_{(n_P)}$. Further it is located in a neighborhood $\mathcal{E}$ of in total $n_\mathcal{E}$ singular divisors. The ordering of the divisors Δ_i, $i < n_P$ is chosen such that the path on which we approach P lies in the growth sector eq. (3.21). The location of the singularity in the enhancement chain is again indicated by boldface:

$$A_1 \to \cdots \to \boldsymbol{A_{(n_P)}} \to \cdots \to A_{(n_\mathcal{E})} \tag{3.17}$$

Enhancement	Tower	Remark
$\mathbf{I}_{\boldsymbol{a},\boldsymbol{b}} \to \mathrm{I}_{\tilde{a},\tilde{b}} - \mathrm{V}_{\tilde{a},\tilde{b}}$	c	type F state
$\mathrm{I}_{a,b} \to \mathbf{I}_{\tilde{\boldsymbol{a}},\tilde{\boldsymbol{b}}}$	x	
$\mathrm{I}_{a,b} \to \mathbf{II}_{\tilde{\boldsymbol{a}},\tilde{\boldsymbol{b}}}$	x	
$\mathrm{I}_{a,b} \to \mathbf{III}_{\tilde{\boldsymbol{a}},\tilde{\boldsymbol{b}}}$	x	
$\mathrm{I}_{a,b} \to \mathbf{IV}_{\tilde{\boldsymbol{a}},\tilde{\boldsymbol{b}}}$	✓	
$\mathrm{I}_{a,b} \to \mathbf{V}_{\tilde{\boldsymbol{a}},\tilde{\boldsymbol{b}}}$	✓	
$\mathbf{II}_{\boldsymbol{a},\boldsymbol{b}} \to \mathrm{II}_{\tilde{a},\tilde{b}}$	c	maybe type F state
$\mathrm{II}_{a,b} \to \mathbf{II}_{\tilde{\boldsymbol{a}},\tilde{\boldsymbol{b}}}$	x	
$\mathbf{II}_{\boldsymbol{a},\boldsymbol{b}} \to \mathrm{III}_{\tilde{a},\tilde{b}}$	✓	
$\mathrm{II}_{a,b} \to \mathbf{III}_{\tilde{\boldsymbol{a}},\tilde{\boldsymbol{b}}}$	x	
$\mathrm{II}_{a,b} \to \mathrm{IV}_{\tilde{a},\tilde{b}}$	✓	
$\mathrm{II}_{a,b} \to \mathrm{V}_{\tilde{a},\tilde{b}}$	✓	
$\mathbf{III}_{\boldsymbol{a},\boldsymbol{b}} \to \mathrm{III}_{\tilde{a},\tilde{b}}$	c	maybe type F state
$\mathrm{III}_{a,b} \to \mathbf{III}_{\tilde{\boldsymbol{a}},\tilde{\boldsymbol{b}}}$	x	
$\mathrm{III}_{a,b} \to \mathrm{IV}_{\tilde{a},\tilde{b}}$	✓	
$\mathrm{III}_{a,b} \to \mathrm{V}_{\tilde{a},\tilde{b}}$	✓	
$\mathrm{IV}_{a,b} \to \mathrm{IV}_{\tilde{a},\tilde{b}}$	✓	
$\mathrm{IV}_{a,b} \to \mathrm{V}_{\tilde{a},\tilde{b}}$	✓	
$\mathrm{V}_{a,b} \to \mathrm{V}_{\tilde{a},\tilde{b}}$	✓	

Table 3.1: Singularity enhancement patterns and whether it is possible to identify an infinite, massless tower of BPS-D4-branes for them. How to construct the towers and which conditions they need to fulfill is described in section 3.3. Boldface indicates on which side of the enhancement the singular point lies; if there is no boldface, both cases are possible. '✓' indicates that it was possible to identify a tower, 'x' that it was not possible and 'c' that there are further conditions on the subindices of the types for the identification to be possible. For the first conditional seed charge it was possible to show that it is a type F state and therefore not suitable for the construction of the infinite tower (see the text for mote details). The other two conditional states as also suspected to be type F states, mainly because they are not expressible through $\tilde{\mathbf{a}}_0^{(2)}$. The results match the ones of the general divisor analysis of section 3.4 and table 3.2; expressions for the $\mathbf{q}_0$s can be read off from there.

A general enhancement chain is now given by

$$\begin{aligned}\mathrm{I}_{a_1,b_1} \to \cdots \to \mathrm{I}_{a_k,b_k} \to \mathrm{II}_{a_{k+1},b_{k+1}} \to \cdots \to \mathrm{II}_{a_m,b_m} \to \mathrm{III}_{a_{m+1},b_{m+1}} \to \cdots \to \mathrm{III}_{a_n,b_n} \to \\ \mathrm{IV}_{a_{n+1},b_{n+1}} \to \cdots \to \mathrm{IV}_{a_o,b_o} \to \mathrm{V}_{a_{o+1},b_{o+1}} \to \cdots \to \mathrm{V}_{a_p,b_p}\end{aligned} \tag{3.18}$$

with P located at any of the divisors. It will turn out that the indices a and b of the divisor types are not required in the following and it suffices to focus on the numerical types I–V. Furthermore we combine multiple consecutive divisors of the same numerical type into the shorthand notation

$$\begin{aligned}\mathrm{I} &\equiv \mathrm{I}_{a_1,b_1} \to \cdots \to \mathrm{I}_{a_k,b_k} \\ \mathrm{II} &\equiv \mathrm{II}_{a_{k+1},b_{k+1}} \to \cdots \to \mathrm{II}_{a_m,b_m} \\ \mathrm{III} &\equiv \mathrm{III}_{a_{m+1},b_{m+1}} \to \cdots \to \mathrm{III}_{a_n,b_n} \\ \mathrm{IV} &\equiv \mathrm{IV}_{a_{n+1},b_{n+1}} \to \cdots \to \mathrm{IV}_{a_o,b_o} \\ \mathrm{V} &\equiv \mathrm{V}_{a_{o+1},b_{o+1}} \to \cdots \to \mathrm{V}_{a_p,b_p}\end{aligned} \tag{3.19}$$

Similar to as before, the general charge orbit is now defined as

$$\mathbf{Q}(\mathbf{q}_0; m_1, \ldots, m_{n_\mathcal{E}}) = \exp\left(\sum_{j=1}^{n_\mathcal{E}} m_j N_j^-\right)\mathbf{q}_0 \tag{3.20}$$

for some seed charge $\mathbf{q}_0$. For the orbit to be infinite, one of the terms $N_i^-\mathbf{q}_0$ has to be non-zero. In this section, we will show however the equivalent condition $N_{(i)}^-\mathbf{q}_0 \neq 0$ for some $i \in \{1, \ldots, n_\mathcal{E}\}$, with $N_{(i)}^- = N_1^- + \cdots + N_i^-$.

As stated, the ordering of the divisors is chosen in such a way that the path we are approaching P on lies within the growth sector

$$\frac{y_1}{y_2}, \frac{y_2}{y_3}, \ldots, \frac{y_{n_P-1}}{y_{n_P}}, y_{n_P} > \lambda \quad \text{and} \quad x_1, \ldots, x_{n_P} < \delta\,, \tag{3.21}$$

where λ and δ are fittingly chosen constants.

For a path in this sector we can now estimate the growth of a flat section $\mathbf{v}$ as we approach the singularity. If $\mathbf{v} \in Gr_{4+l_1}^{(1)} \cap \cdots \cap Gr_{4+l_{n_P}}^{(n_P)}$ then its leading order growth as $y_i \to \infty$ is

$$\|\mathbf{v}\|^2 \sim \left(\frac{y_1}{y_2}\right)^{l_1}\left(\frac{y_2}{y_3}\right)^{l_2} \ldots (y_{n_P})^{l_{n_P}} \tag{3.22}$$

In summary, a suitable seed charge $\mathbf{q}_0$ has to fulfill the properties

$$N_i^-\mathbf{q}_0 \neq 0 \quad \text{for at least one } i \in \{1, \ldots, n_\mathcal{E}\} \tag{3.23}$$

$$l_1, \ldots, l_{n_P-1} \leq 0 \quad \text{and} \quad l_{n_P} < 0 \tag{3.24}$$

Table 3.2 lists the suiting seed charges for all enhancement chains where this is possible. We will now discuss in turn that these are indeed satisfying the infiniteness and masslessness condition.

Enhancement Chain	$\mathbf{q}_0$
$\dots \to \mathbf{II} \to \mathrm{III/IV/V} \to \dots$	$N_{(n_P)}\tilde{\mathbf{a}}_0^{(n\varepsilon)}$
$\dots \to \mathbf{III} \to \mathrm{IV/V} \to \dots$	$(N_{(n_P)})^2\tilde{\mathbf{a}}_0^{(n\varepsilon)}$
$(\mathrm{I} \to)\ \mathbf{IV} \to \dots$	$(N_{(n_P)})^2\tilde{\mathbf{a}}_0^{(n\varepsilon)}$
$\dots \to \mathrm{II} \to \mathbf{IV} \to \dots$	$N_{(n_P)}N^-_{(m)}\tilde{\mathbf{a}}_0^{(n\varepsilon)}$
$\dots \to \mathrm{III} \to \mathbf{IV} \to \dots$	$(N^-_{(n)})^2\tilde{\mathbf{a}}_0^{(n\varepsilon)}$
$(\mathrm{I} \to)\ (\mathrm{IV} \to)\ \mathbf{V}$	$(N_{(n_P)})^3\tilde{\mathbf{a}}_0^{(n\varepsilon)}$
$\dots \to \mathrm{II} \to (\mathrm{IV} \to)\ \mathbf{V}$	$(N_{(n_P)})^2N^-_{(m)}\tilde{\mathbf{a}}_0^{(n\varepsilon)}$
$\dots \to \mathrm{III} \to (\mathrm{IV} \to)\ \mathbf{V}$	$N_{(n_P)}(N^-_{(n)})^2\tilde{\mathbf{a}}_0^{(n\varepsilon)}$

Table 3.2: Enhancement chains, with location of the singular point indicated by boldface, for which an infinite, massless tower can be constructed. In the enhancement chains the shorthand notation of eq. (3.19) was used. Singularity types in parentheses can be present in the chain but do not have to. The seed charge $\mathbf{q}_0$ for the construction of section 3.4 is expressed in terms of $\tilde{\mathbf{a}}_0^{(n\varepsilon)}$ where possible. $N^-_{(m)}$ denotes the N^- assigned to the last type II divisor and $N^-_{(n)}$ denotes the N^- assigned to the last type III divisor, see eq. (3.18).

Infiniteness of the general charge orbit. For the cases where P lies on a type II divisor, there has to be a type III, IV or V divisor higher up in the enhancement chain. Let us say the first of these is at position j. Then the $N^-_{(j)}$ associated to this divisor is not annihilating the proposed $\mathbf{q}_0$. This can be seen by noting that for III, IV and V we have $(N^-)^2\tilde{\mathbf{a}}_0^{(n\varepsilon)} \neq 0$ as can be read of from the prospective diamonds (see table 2.1). From this it follows that $N^-_{(j)}\mathbf{q}_0 \neq 0$ and therefore that the orbit is infinite.

A similar argument holds for the case that P lies on a type III divisor. Denote the position of the first IV or V divisor higher up in the chain again by j. Then, because for these two types we have $(N^-)^3\tilde{\mathbf{a}}_0^{(n\varepsilon)} \neq 0$, it follows that $N^-_{(j)}\mathbf{q}_0 \neq 0$ and in turn that the orbit is infinite.

For the type IV case, it immediately follows from $(N_{(n_P)})^3\tilde{\mathbf{a}}_0^{(n\varepsilon)} \neq 0$ that $N_{(n_P)}\mathbf{q}_0 \neq 0$ and similarly, for the V case, $(N_{(n_P)})^4\tilde{\mathbf{a}}_0^{(n\varepsilon)} \neq 0$ implies likewise $N_{(n_P)}\mathbf{q}_0 \neq 0$. Both cases have therefore infinite orbits.

Masslessness of the general charge orbit. The condition for masslessness from eq. (3.24) can be shown by tracking the location of the respective $\mathbf{q}_0$s through the enhancement chains. We do this by looking at the evolution of the primitive spaces $P^{(i)}_{n+l}$ across enhancements, using their definition eq. (2.36), the fact that $N^-_{(i+1)} = N^-_{(i)} + N^-_{i+1}$ and the well defined mapping behavior of N^-_{i+1}. With this we can for example deduce that for all enhancements $A_{(i)} \to A_{(i+1)}$ we have

$$P_n^{(i+1)} + N_{(i+1)}^- P_{n+1}^{(i+1)} + (N_{(i+1)}^-)^2 P_{n+2}^{(i+1)} \subset P_n^{(i)} + N_{(i)}^- P_{n+1}^{(i)} + (N_{(i)}^-)^2 P_{n+2}^{(i)} \,. \tag{3.25}$$

Theses three spaces lie furthermore all on or below the diagonal, i.e.

$$P_n^{(i)} + N_{(i)}^- P_{n+1}^{(i)} + (N_{(i)}^-)^2 P_{n+2}^{(i)} \subset Gr_n^{(i)} + Gr_{n-1}^{(i)} + Gr_{n-2}^{(i)} \,. \tag{3.26}$$

We can now make direct use of this for P on a type II divisor. There $\mathbf{q}_0 \in N_{(n_P)}^- P_{n+1}^{(n_P)}$ and therefore $l_{n_P} = -1$. Additionally, because of eq. (3.25), we also have $\mathbf{q}_0 \in P_n^{(i)} + N_{(i)}^- P_{n+1}^{(i)} + (N_{(i)}^-)^2 P_{n+2}^{(i)}$ and hence $l_i \leq 0$ with $i < n_P$. This shows that $\mathbf{q}_0$ fulfills eq. (3.24) and that the orbit is massless.

Similarly, for P on a type III divisor, we have $\mathbf{q}_0 \in (N_{(n_P)}^-)^2 P_{n+2}^{(n_P)}$ and hence $l_{n_P} = -2$. Again eq. (3.25) tells us then that $l_i \leq 0$ with $i < n_P$ and hence that the orbit is massless.

For type IV and V singular points the discussion gets more involved. For P on a IV divisor, in all three cases of table 3.2 we have $\mathbf{q}_0 \in (N_{(n_P)}^-)^2 P_{n+3}^{(n_P)}$ and $l_{n_P} = -1$. $\mathbf{q}_0$ stays below the diagonal in type IV diamonds further down the chain because for $\mathrm{IV}_{(i)} \to \mathrm{IV}_{(i+1)}$ enhancements we have the invariance

$$(N_{(i+1)}^-)^2 P_{n+3}^{(i+1)} \subset (N_{(i)}^-)^2 P_{n+3}^{(i)} \,. \tag{3.27}$$

In the first case of table 3.2 either there is no divisor with type smaller than IV. Then the masslessness condition is satisfied. If there is a type I divisor then we have for the $\mathrm{I}_{(i)} \to \mathrm{IV}_{(i+1)}$ enhancement

$$(N_{(i+1)}^-)^2 P_{n+3}^{(i+1)} \subset P_n^{(i)} \tag{3.28}$$

which gives $l_i = 0$ and together with eq. (3.25) likewise the masslessness of the orbit. In the second case we have at the $\mathrm{II}_{(i)} \to \mathrm{IV}_{(i+1)}$ enhancement

$$(N_{(i+1)}^-)^2 P_{n+3}^{(i+1)} \subset P_{n+1}^{(i)} + N_{(i)}^- P_{n+1}^{(i)} \,. \tag{3.29}$$

$P_{n+1}^{(i)}$ would pose now a problem. However, the particular construction of $\mathbf{q}_0$ for this case ensures that $\mathbf{q}_0 \in N_{(i)}^- P_{n+1}^{(i)}$. And again, eq. (3.25) guarantees that $\mathbf{q}_0$ stays on or below the diagonal and hence that the orbit is massless. Similarly, in the third case we have at the $\mathrm{III}_{(i)} \to \mathrm{IV}_{(i+1)}$ enhancement

$$(N_{(i+1)}^-)^2 P_{n+3}^{(i+1)} \subset N_{(i)}^- P_{n+2}^{(i)} + (N_{(i)}^-)^2 P_{n+2}^{(i)} \,, \tag{3.30}$$

where the first term on the right side poses a problem which is however fixed by the particular construction of $\mathbf{q}_0$. It keeps $\mathbf{q}_0 \in (N_{(i)}^-)^2 P_{n+2}^{(i)}$ and together with eq. (3.25) this gives the masslessness of the orbit.

Lastly, for P on a type V divisor, we have in all three cases $\mathbf{q}_0 \in (N_{(n_P)}^-)^3 P_{n+4}^{(n_P)}$ giving $l_{n_P} = -2$. If there is no type IV divisor in the chain then the discussion is exactly the one for P on a type IV divisor with every occurrence of type IV replaced by type V and $(N^-_{(i)})^2 P^{(i)}_{n+3}$ replaced by $(N^-_{(i)})^3 P^{(i)}_{n+4}$. If there is however a type IV divisor in the chain then, due to $(N^-_{(i)})^3 P^{(i+1)}_{n+4} \subset (N^-_{(i)})^2 P^{(i)}_{n+3}$ at the $\mathrm{IV}_{(i)} \to \mathrm{V}_{(i+1)}$ enhancement, the discussion for the type IV divisor can be repeated again. For brevity we will not do this.

This concludes the prove that indeed all seed charges in table 3.2 produce infinite and massless orbits.

3.5 Replacing N^- with N in the charge orbit

We were able to construct charge orbits for a variety of general enhancement patterns. However, for this we were making use of the special $\mathfrak{sl}_2$ basis, which is quite difficult to compute for explicit examples. It is desirable to express the charge orbit in terms of the original basis, i.e. in terms of the N_i and $\mathbf{a}_0$ instead of N_i^- and $\tilde{\mathbf{a}}_0^{(n_\mathcal{E})}$. In this section I want to show that this is at least possible for the exponential factor in the charge orbit.

Explicitly the claim is that the modified charge orbit (compare the use of N_j with eq. (3.20))

$$\mathbf{Q}'(\mathbf{q}_0; m_1, \ldots, m_{n_\mathcal{E}}) = \exp\left(\sum_{j=1}^{n_\mathcal{E}} m_j N_j\right)\mathbf{q}_0 \tag{3.31}$$

is still infinite and massless for each of the $\mathbf{q}_0$s from table 3.2.

To show this we first decompose each N_i as

$$N_i = \sum_{s\in\mathbb{Z}} N_i^{[s]} \quad \text{with} \quad N_i^{[s]} Gr_l^{(i-1)} \subset Gr_{l+s}^{(i-1)} \,. \tag{3.32}$$

This is a crucial step in the construction of the $\mathfrak{sl}_2$ basis of [19] and it is shown there that it is always well defined. Actually the N_i^- are defined as $N_i^- \equiv N_i^{[0]}$. As a first corollary from this it follows that if $N_i^- \mathbf{q}_0 \neq 0$ then $N_i \mathbf{q}_0 \neq 0$, showing the claimed infiniteness of the modified charge orbit.

We can furthermore deduce that in the expansion eq. (3.32) only the terms with $s \leq 0$ are non-zero. To see this, note that all N_i are commuting and leave thus the image and kernel of each other invariant. From the definition of the $W_l^{(i)}$ in terms of these spaces (see eq. (2.19)) it follows that $N_i W_l^{(j)} \subset W_l^{(j)}$ and hence that $N_i Gr_l^{(j)} \subset \bigoplus_{s\leq 0} Gr_{l+s}^{(j)}$. This means that the N_i can only keep the value of each l_j the same or reduce it, but cannot increase it. Hence if a seed charge fulfills the masslessness condition eq. (3.24) then the modified charge orbit fulfills the condition as well and the claim is proven.

4 Conclusion

In this thesis we analyzed the Swampland Distance Conjecture in the complex structure moduli space of Calabi-Yau fourfolds. The conjecture (see section 1.1) states that at infinite distance points in moduli space an infinite tower of massless states emerges. We studied in turn the two ingredients of this statement, the infinite distance points and the tower of states, for fourfold compactifications.

Firstly, a very general analysis of degeneration points of fourfolds was done within the powerful framework of Hodge theory. A classification of these points was simplified greatly by assigning mixed Hodge structures to them, which depend on the complex structure and monodromy transformations associated to the degeneration points. The mixed Hodge structures are represented by their Deligne splitting which could be classified by looking at their corresponding Deligne diamonds. This classification results in five different main types, enumerated by Roman numerals I–V, each further supplemented by two numeric indices; table 2.1 lists the full result, including the constraints on the numeric indices. Together with results of [21], it was then possible to identify the infinite distance points among the degeneration points. Besides classifying the degeneration points into different types, we also looked at how these local structures are connected and what types can occur when two degenerations combine and enhance to a multi parameter degeneration. The conditions on the types before and after such an enhancement can be found in table 2.2. With this we started to unravel a global picture of an infinite distance network in moduli space.

The second ingredient for showing the Swampland Distance Conjecture was then to construct infinite towers of massless states in the form of what we termed *charge orbits*. In [6] the authors argued that for Calabi-Yau threefolds and one parameter degenerations such charge orbits are populated by BPS D-brane states. We assumed that this also holds for fourfolds and the multi parameter case; the proof will be left for future work. At first, we then looked at one parameter degenerations, where it was possible to identify fitting charge orbits for type IV and type V degenerations. Next, we analyzed respectively two parameter and arbitrary multi parameter degenerations. In both cases it was again possible to find a charge orbit if the degeneration was of type IV or V, whereas for type II and III this was only possible if somewhere in the neighborhood the degeneration further enhances into one with a greater numerical type. A desirable continuation of this work would be to identify fitting charge orbits without this constraint. In summary, we succeeded however in providing further evidence for the Swampland Distance Conjecture for Calabi-Yau fourfold compactifications of type IIA string theory.

In the derivations leading to the aforementioned results we used a special $\mathfrak{sl}_2$-basis that was introduced by [19] and reviewed in [12]. Because this basis is difficult to construct, we gave an argument in section 3.5 that it is also possible to define a modified charge orbit using the original basis. However, we were not able to remove the dependence on the $\mathfrak{sl}_2$-basis completely; it is still needed for the identification of the seed charges, even for the modified charge orbits.

Even though the main goal of this thesis was to provide the mentioned evidence for the SDC, the presented classification of singular fourfolds and enhancements between them is an important result on its own. It depends only on general properties of Calabi-Yau manifolds and is therefore expected to be transferable to scenarios other than compactifications of type IIA theory. One such scenario of interest would be, for example, F-theory compactified on a fourfold. Another aspect to be noted is that even though we only looked at the complex structure moduli space we can use mirror symmetry between Calabi-Yaus manifolds to map the results to the Kähler moduli space. Lastly, a second application of the developed tools and results could be to estimate the number and distribution of flux vacua around infinite distance points as a continuation of the work of Denef and Douglas [23].

Bibliography

[1] E. Palti. "The Swampland: Introduction and Review". In: (Mar. 14, 2019) (cit. on pp. 4, 6).

[2] H. Ooguri and C. Vafa. "On the Geometry of the String Landscape and the Swampland". In: *Nuclear Physics B* 766.1-3 (Mar. 2007), pp. 21–33. arXiv: `hep-th/0605264` (cit. on p. 4).

[3] S. Brahma and M. W. Hossain. "Relating the Scalar Weak Gravity Conjecture and the Swampland Distance Conjecture for an Accelerating Universe". In: (Apr. 11, 2019). arXiv: `1904.05810 [gr-qc, physics:hep-th]` (cit. on p. 4).

[4] T. W. Grimm and D. van de Heisteeg. "Infinite Distances and the Axion Weak Gravity Conjecture". In: (May 2, 2019). arXiv: `1905.00901 [hep-th]` (cit. on p. 4).

[5] H. Ooguri et al. "Distance and de Sitter Conjectures on the Swampland". In: *Physics Letters B* 788 (Jan. 2019), pp. 180–184. arXiv: `1810.05506` (cit. on pp. 4, 5).

[6] T. W. Grimm, E. Palti, and I. Valenzuela. "Infinite Distances in Field Space and Massless Towers of States". In: *Journal of High Energy Physics* 2018.8 (Aug. 2018). arXiv: `1802.08264` (cit. on pp. 4, 5, 28, 40).

[7] R. Blumenhagen. "Quantum Gravity Constraints on Large Field Inflation". In: *Proceedings of Corfu Summer Institute 2017 "Schools and Workshops on Elementary Particle Physics and Gravity" — PoS(CORFU2017)*. Corfu Summer Institute 2017 "Schools and Workshops on Elementary Particle Physics and Gravity". Vol. 318. SISSA Medialab, Aug. 24, 2018, p. 175 (cit. on pp. 4, 5).

[8] F. Baume and E. Palti. "Backreacted Axion Field Ranges in String Theory". In: *J. High Energ. Phys.* 2016.8 (Aug. 2016), p. 43. arXiv: `1602.06517` (cit. on pp. 4, 5).

[9] D. Klaewer and E. Palti. "Super-Planckian Spatial Field Variations and Quantum Gravity". In: *J. High Energ. Phys.* 2017.1 (Jan. 2017), p. 88. arXiv: `1610.00010` (cit. on pp. 4, 5).

[10] R. Blumenhagen et al. "The Refined Swampland Distance Conjecture in Calabi-Yau Moduli Spaces". In: *J. High Energ. Phys.* 2018.6 (June 2018), p. 52. arXiv: `1803.04989` (cit. on pp. 4, 5).

[11] S. Cecotti. *Supersymmetric Field Theories: Geometric Structures and Dualities*. Cambridge: Cambridge University Press, 2015 (cit. on pp. 4, 5).

[12] T. W. Grimm, C. Li, and E. Palti. "Infinite Distance Networks in Field Space and Charge Orbits". In: (Nov. 6, 2018). arXiv: `1811.02571 [hep-th]` (cit. on pp. 4, 5, 17, 21, 24, 28, 31, 40).

[13] P. Corvilain, T. W. Grimm, and I. Valenzuela. “The Swampland Distance Conjecture for Kähler Moduli”. In: (Dec. 18, 2018). arXiv: 1812.07548 [hep-th] (cit. on p. 4).

[14] R. Blumenhagen, I. Valenzuela, and F. Wolf. “The Swampland Conjecture and F-Term Axion Monodromy Inflation”. In: *J. High Energ. Phys.* 2017.7 (July 2017), p. 145. arXiv: 1703.05776 (cit. on p. 4).

[15] M. Graña and H. Triendl. *String Theory Compactifications*. New York, NY: Springer Berlin Heidelberg, 2017 (cit. on p. 7).

[16] A. Klemm et al. “Calabi-Yau Fourfolds for M- and F-Theory Compactifications”. In: *Nuclear Physics B* 518.3 (May 1998), pp. 515–574. arXiv: hep-th/9701023 (cit. on p. 9).

[17] M. Haack. “Calabi-Yau Fourfold Compactifications in String Theory” (cit. on p. 10).

[18] C. Robles. “Degenerations of Hodge Structure”. In: (July 4, 2016) (cit. on pp. 13, 21).

[19] E. Cattani, A. Kaplan, and W. Schmid. “Degeneration of Hodge Structures”. In: *Annals of Mathematics* 123.3 (1986), pp. 457–535 (cit. on pp. 17, 30, 39, 40).

[20] M. Kerr, G. Pearlstein, and C. Robles. “Polarized Relations on Horizontal SL(2)s”. In: (May 8, 2017). arXiv: 1705.03117 [math] (cit. on pp. 19, 21, 24).

[21] C.-L. Wang. “On the Incompleteness of the Weil-Petersson Metric along Degenerations of Calabi-Yau Manifolds”. In: *Math. Res. Lett.* 4.1 (Jan. 1997), pp. 157–171 (cit. on pp. 21, 40).

[22] C.-L. Wang. “Aspects on Calabi-Yau Moduli”. In: *Uniformization, Riemann-Hilbert Correspondence, Calabi-Yau Manifolds & Picard-Fuchs Equations*. International Press, 2018 (cit. on p. 21).

[23] F. Denef and M. R. Douglas. “Distributions of Flux Vacua”. In: *J. High Energy Phys.* 2004.05 (May 28, 2004), pp. 072–072. arXiv: hep-th/0404116 (cit. on p. 41).